

# Inferring central McArthur Basin shape at HYC time: Integration of geophysical interpretation and geology using GIS

ML Duffett<sup>1, 2</sup>, M Roach<sup>1</sup> and DE Leaman<sup>1, 3</sup>

Sediment-hosted metallogeny results from sedimentary basin fluid flow, which in turn, is controlled by the evolving architecture of the basin. Understanding and predicting the location of ore deposits therefore depends on knowledge of the three-dimensional geometry of the target basin through time (4-D basin architecture). However, quantitative basin analysis is severely handicapped in the absence of extensive seismic reflection data from the target terranes, such as the Proterozoic of northern Australia, host to a world-class base metal endowment. Geological mapping and regional potential field geophysical data, on the other hand, are widely available, but their interpretation in terms of 4-D basin architecture is not straightforward. GIS and geophysical modelling were deployed to assist.

A GIS with 1:250 000-scale geological map and geochemical data was designed and implemented for a region in the McArthur Basin encompassing the giant HYC Zn-Pb-Ag deposit. The GIS incorporates geological attributes that encode depth information implicit in the stratigraphic column. This data structure, in conjunction with topological attributes, allows queries based on the stratigraphic relationships of spatial elements.

An initial 3-D picture of the basin, relying solely on surface geological data and measured stratigraphic thicknesses, was developed by generation of layers comprising ‘predicted’ structure contour values for any given stratigraphic unit. This prediction is analogous to calculation of the theoretical Bouguer gravity value during reduction of gravity data. The predicted value (for example, of basement depth) does not necessarily indicate the true elevation of the surface being considered at a given location; rather, it is a baseline for comparison. Lateral variations from this baseline indicate departures of basin shape from ‘layer-cake’ geometry. By this mechanism, elements of the basin fill, lost due to deformation and erosion following terminal deposition, may be restored for comparative purposes.

The development of stratigraphic topology enables automatic identification of the location and magnitude of unconformities on geological maps. These indicate areas and periods of uplift through the sedimentation history of the basin, from which fluid flow may have been topographically driven. Conversely, the distribution of unconformities circumscribes regions of more continuous sedimentation, where accommodation space was developed more consistently.

Both gravity and magnetic data were forward modelled in an extensive interlocking array of cross-sectional 2-D profiles. Several basin units are resolvable

from regional data using these methods. In particular, the HYC-hosting upper McArthur Group is distinguishable due to its carbonate-dominant composition, resulting in a positive density contrast. These interpretations, initially expressed as structure contours and isopachs (Leaman 1998), were interpolated into 3-D models of the present disposition of basin units. These may be compared directly with the basin unit depths and thicknesses ‘predicted’ from outcrop-derived data.

Residuals, after removal of ‘predicted’ or ‘layer-cake’ McArthur Group thickness from the ‘actual’ (geophysically interpreted) present thickness, directly map the location and size of active sub-basins at the time of the formation of HYC mineralisation. The sub-basins thus defined are congruent with indications from unconformity distribution. HYC’s situation at the northeastern edge of one of these sub-basins is consistent with topographic and bounding growth fault control on the palaeohydrogeological regime that focused mineralising fluids in the vicinity of the deposit. Other sub-basin edges are indicated as sites of potential base metal mineralisation.

**Keywords:** Northern Territory, McArthur Basin, geographic information systems, sedimentary basins, reconstruction, mineral deposits, metallogenesis, SEDEX, exhalative processes, base metals, geophysical interpretation, geological interpretation

## INTRODUCTION

Stratiform Zn-Pb deposits occurring in the Palaeoproterozoic and earliest Mesoproterozoic sedimentary successions of northern Australia represent one of the largest accumulations of base metals known in Earth’s crust. Examples include the giant deposits of Mount Isa, Century and McArthur River (HYC). Natural sedimentary basin processes, operating to form these deposits, concentrated tens of millions of tonnes of base metals at several orders of magnitude over average crustal concentration. An exceptional combination of geological circumstances, encompassing a large volume of rock, is indicated, which incorporates (following Wyborn *et al* 1995):

- a source for the metals
- a solvent (probably basinal brines) to carry them
- aquifers (permeable strata or fracture systems) to provide a conduit and focusing mechanism for the metal-bearing fluid
- suitable host rock, probably reduced carbonaceous fine-grained sediments, to sequester the metals from the basin brine into the sedimentary succession in ore-level concentrations (upwards of 10% by weight).

Model-based prediction of where other large Zn-Pb orebodies might occur is thus a four-dimensional problem requiring knowledge, not only of structures governing where

<sup>1</sup> Centre for Ore Deposit Research, University of Tasmania, GPO Box 252–79, Hobart TAS 7001.

<sup>2</sup> formerly Northern Territory Geological Survey, PO Box 8760, Alice Springs, NT, 0871.

<sup>3</sup> Leaman Geophysics, GPO Box 320, Hobart TAS 7001.

metal-bearing fluids might have been focused to intersect a stratum of reducing sediment, but also when the special conjunction of factors existed to permit this to occur. All this must be evaluated within the context of a sedimentary basin – a dynamic, continually evolving, three-dimensional system. A primary issue in predicting deposit location is hence to reconstruct basin geometry as it was when the mineralisation event(s) occurred over 1600 million years ago; not as it is now, several deformation events and erosion episodes later.

This paper presents some GIS-based approaches to the problem of reconstructing north Australian Proterozoic basin architecture. The region containing the HYC deposit, the central-southern Batten Fault Zone of the McArthur Basin, was chosen for evaluation (**Figure 1**).

It was soon recognised that approaches involving empirical spatial correlation of base metal deposit occurrences with various geological factors (eg Bonham-Carter 1990) were unlikely to be fruitful. A primary reason for this is the small number of significant known orebodies available to ‘train’

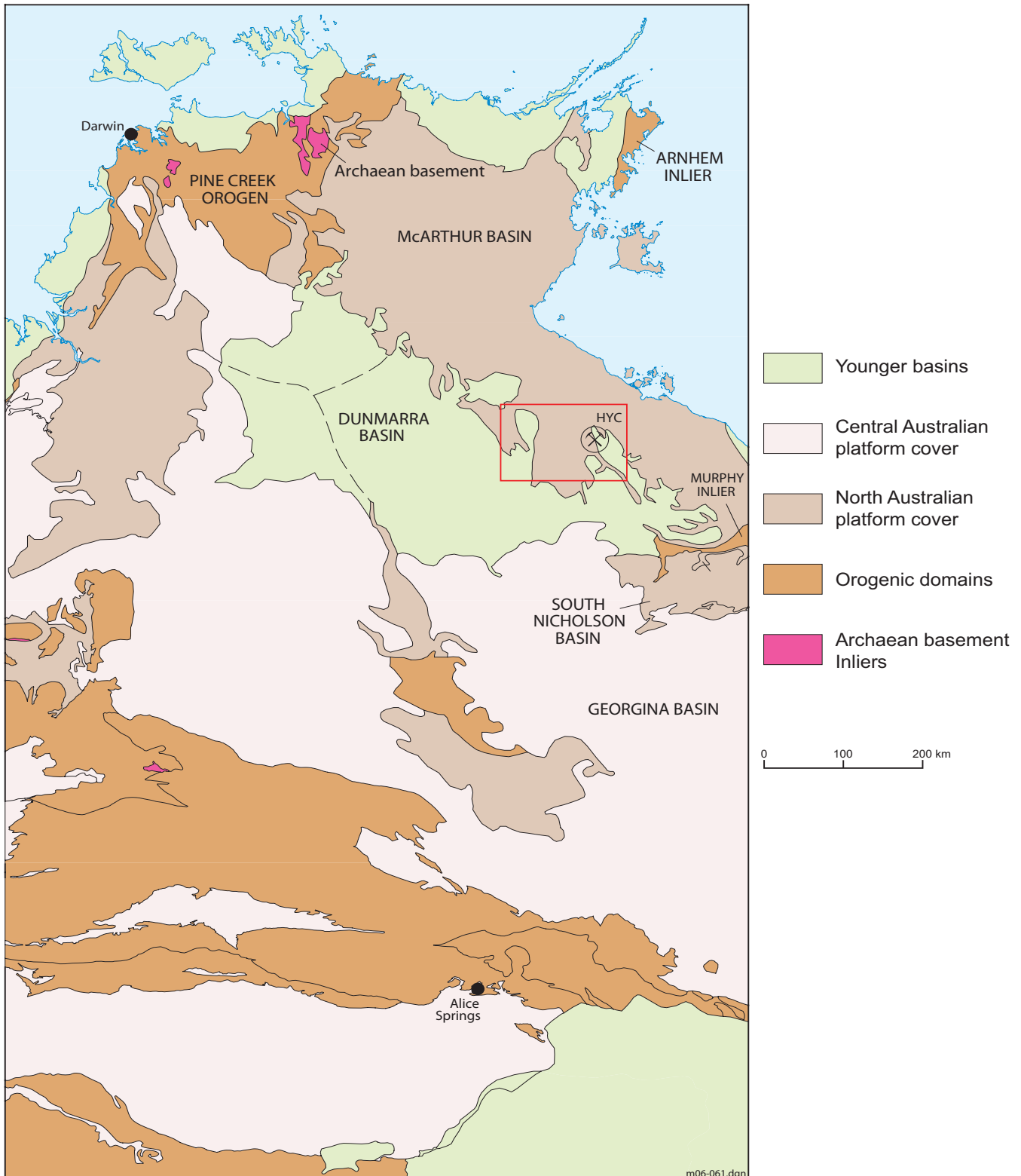


**Figure 1.** Major geological regions of the Northern Territory, with GIS study area outlined in red.

or develop a set of decision rules for such an approach. Another problem is the lack of extensive outcrop in many areas of the Carpentaria Zinc Belt. This is exacerbated by the recessive nature of many of the prospective stratigraphic units, such that prospective host rocks and mineralisation-controlling structures are obscured. This situation is in direct contrast to precious metal provinces in Canada and Western Australia, where GIS has been successfully applied to prospectivity mapping using statistical methods (Wright and Bonham-Carter 1992, Knox-Robinson *et al* 1992). In these areas, economic concentrations of the commodity sought occur in a large number of structurally controlled deposits in well-exposed or easily-geophysically-mappable terrain. Economic stratiform sediment-hosted base metal mineralisation, on the other hand, is typically concentrated in a few major deposits, the spatial controls of which are unclear. A theoretical, essentially model-driven approach has therefore been adopted for this study.

In the rare cases where GIS approaches to stratabound base metal prospectivity mapping have been attempted, such as in Jagodzinski *et al* (1993) and d'Ercole (2000), the spatial controls utilised (major regional faults and reducing 'trap' units) have presumably been identified on both empirical and theoretical grounds. Prospectivity maps that are based on such regional spatial criteria successfully encompass most known base metal occurrences, but are a rather blunt instrument in that the identified prospective area remains quite large in comparison to the extent of the deposits sought and the size of the metallogenic province.

Base metal metallogeny is especially dependent on controls operating in the depth (z) dimension. Of the controls outlined above, metal sources, mineralising fluid migration pathways and mineralisation traps are most amenable to analysis, given the available data. The other systems are either too poorly constrained by the available data, or demand sophisticated fluid modelling techniques beyond the scope of this work (but see, for example, Yang *et al* 2004).

Conventional regional geological data and data models are inadequate to address the metallogenic problems outlined above. The main aims of this work were to redress this; firstly, by presenting results from new techniques developed to extract and visualise information pertinent to four-dimensional base metal metallogeny from standard regional geological data; and secondly, by assessing this information with respect to interpretations of regional geophysical data. The common theme in all these approaches is the extraction of the maximum three-dimensional information from the available data, in order to define the geometry of the host basin. The derived products are used to make inferences concerning the palaeo-geometry of the basin, which will have been a first-order control on the localisation of Zn-Pb mineralisation.

## MCARTHUR BASIN GEOLOGY AND MINERALISATION

The McArthur Basin extends northwest from the Murphy Inlier along the western coast of the Gulf of Carpentaria into eastern Arnhem Land. Only the area of BAUHINIA DOWNS<sup>4</sup> was examined in detail in this work (Figure 1).

The discussion of McArthur Basin stratigraphy below thus focuses on units present in this district. Units of the succession that includes and precedes HYC mineralisation are examined in most detail (Figure 2), as these will have the greatest bearing on metallogenic hypotheses for the deposit. This section of the McArthur Basin is best exposed in central portion of the BAUHINIA DOWNS study area (Figure 3), in the area known as the Batten Fault Zone (or Batten Trough).

The oldest unit exposed in the study area, the Scrutton Volcanics, is dated at  $1857 \pm 30$  Ma (Pietsch *et al* 1991) and comprises basement to the McArthur Basin in this region. It is related to Barramundi Orogeny-related, continent-wide deformation and felsic magmatism (Etheridge *et al* 1987), and consists of thick pyroclastic sheets of K-rich dacitic and rhyodacitic composition, with minor felsic and mafic lavas (Rawlings 1994).

The Tawallah Group represents the Redbank package (Rawlings 1999, 2007), and as such is believed to have a depositional age range of 1815–1705 Ma. It is composed of sandstones, with bimodal igneous intrusions and lavas, lutite, conglomerate and dolostone. Three cycles of sedimentation and igneous activity have been recognised within the Tawallah Group (Rogers 1996), which may represent several superimposed basin phases (Rawlings 1999, 2007).

The carbonate-dominated McArthur Group approximates to the Glyde package (Rawlings 1999) and is correlated with the Fickling, McNamara and Mount Isa groups of the Mount Isa Basin. The Umbolooga Subgroup comprises approximately the lower two-thirds of the McArthur Group in thickness terms. Although sandstone is a relatively minor constituent of the Umbolooga Subgroup, it is most common in its lower portion. Dolostone, usually fine grained, is the most prevalent lithology in the Umbolooga Subgroup. The Batten Subgroup is generally even more dolomitic than the Umbolooga Subgroup. The age of the Batten Subgroup is well constrained by SHRIMP zircon ages of  $1625 \pm 2$  Ma for the Stretton Sandstone and  $1614 \pm 4$  Ma for the Amos Formation (Page *et al* 2000).

The Nathan Group generally overlies the McArthur Group unconformably, although radiometric dates of  $1613 \pm 4$  and  $1609 \pm 3$  Ma (cf Amos Formation, above) and a paraconformable relationship observed near the base of the Nathan Group in the southern portion of the study area led Rawlings (1999) to group this part of the Nathan Group with the McArthur Group, in his basin-wide Glyde package. Elsewhere, basal polymict conglomerate and pebbly lithic (chert) sandstone in the Smythe Sandstone mark the base of the Nathan Group. The remainder of the Nathan Group mainly consists of dolostone contained in the Balbirini Dolostone (up to 1500 m thick) and Dungaminnie Formation (up to 240 m thick), although there are beds of fine sandstone and siltstone in the lower portion of the latter. Thickness variations in the Nathan Group are mostly due to post-depositional erosion. A date of  $1589 \pm 3$  Ma from the middle of the Balbirini Dolostone is held to best represent the age of the main part of the Nathan Group (Rawlings 1999).

The Roper Group is almost entirely siliciclastic, being mainly composed of quartz sandstone with micaceous siltstone (Plumb *et al* 1990). Its base is marked by a regional unconformity developed on the Nathan and McArthur

<sup>4</sup> Names of 1:250 000 mapsheets are in upper case, eg BAUHINIA DOWNS.

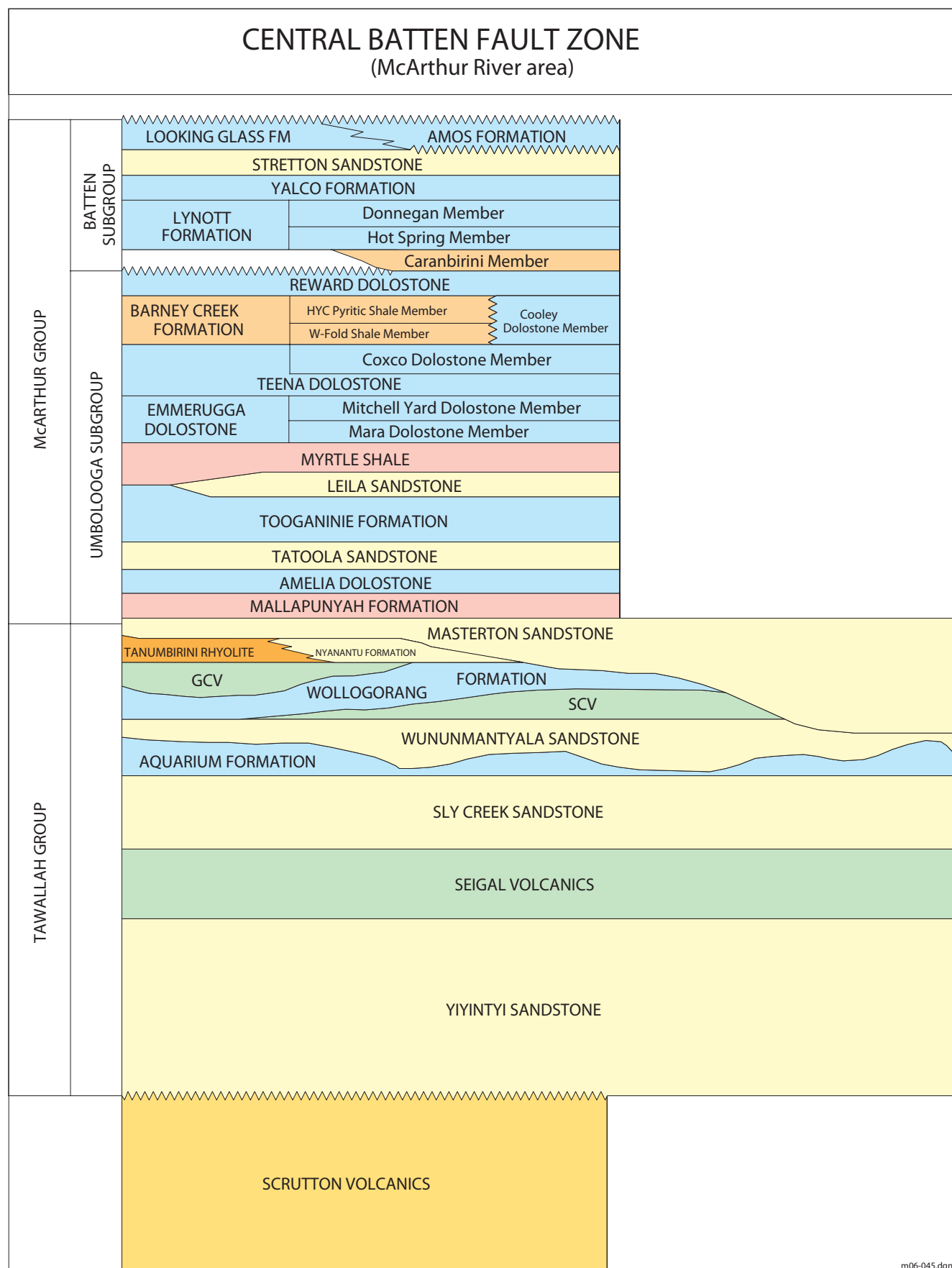


**Figure 2.** Lower McArthur Basin stratigraphy, modified after Pietsch *et al* (1991) and S Bull (pers comm 1998). Units are colour-coded according to dominant composition, with felsic volcanics orange, sandstones yellow, mafic igneous units green, dolostones light blue, oxidised shales and siltstones red and reduced carbonaceous shales and siltstones brown.



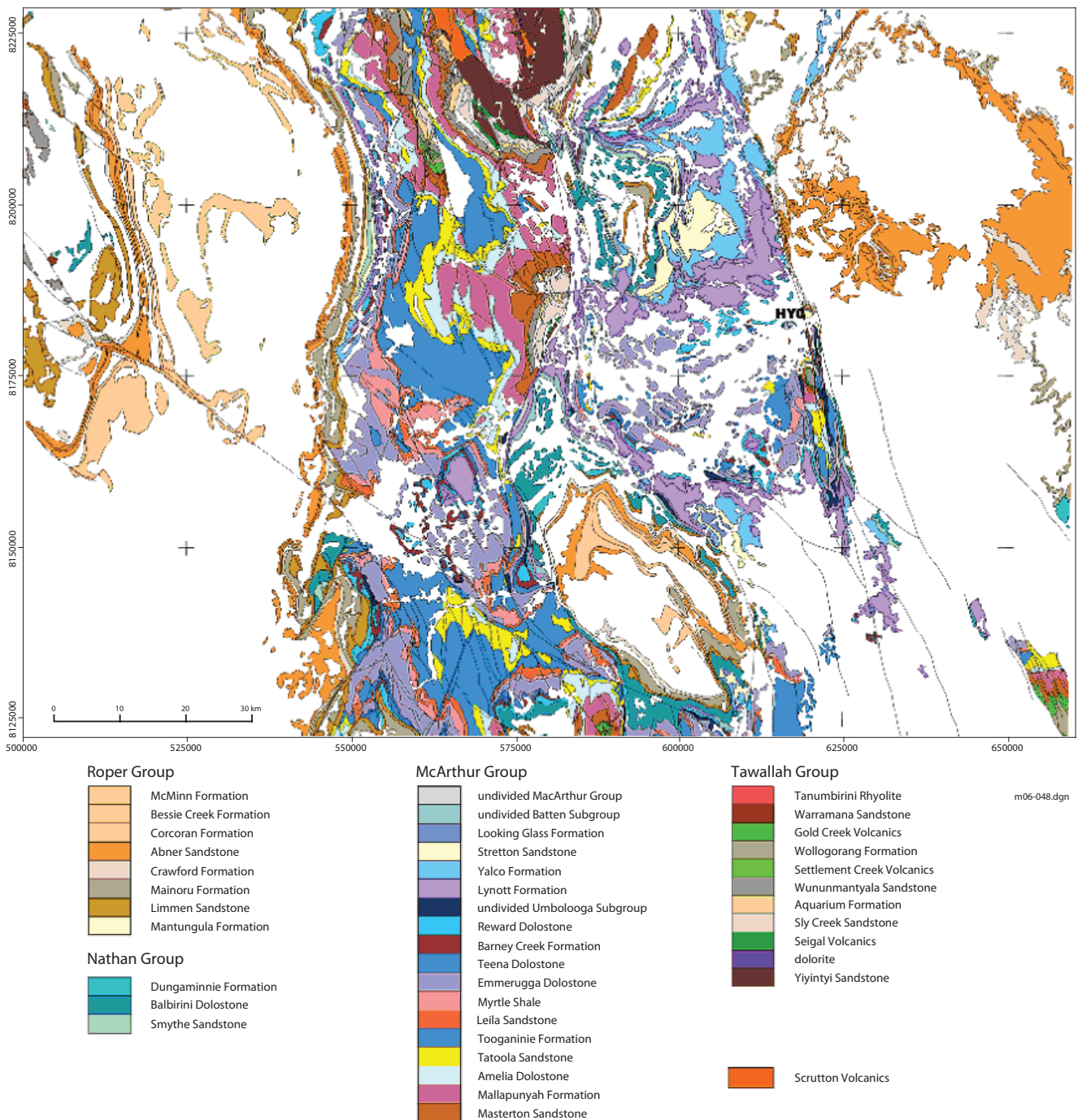


**Figure 3.** Proterozoic geology, BAUHINIA DOWNS study area. Grid coordinates for this and all subsequent maps are of the Australian Map Grid (AGD66), zone 53.

groups. The Roper Group thickens from east to west across the BAUHINIA DOWNS study area, from less than 1 km up to 5 km, marking a substantial shift in depocentre from the earlier McArthur Basin successions (Plumb and Wellman 1987). It consists of nine formations deposited in a series of five upward-coarsening cycles (Jackson *et al* 1988), and characterises the basin-spanning Wilton package of Rawlings (1999). Numerous dolerite and gabbro dykes and sills intrude the Roper Group, but there is no evidence that these are volumetrically significant in the study area. One of these, dated at 1280 Ma (K-Ar), provides an absolute minimum age constraint on the Roper Group, while a minimum age of 1390 Ma is indicated by Rb-Sr dating of glauconite (McDougall *et al* 1965). A diagenetic illite Rb-Sr age of  $1429 \pm 31$  Ma from near the top of the Roper Group

(Kralik 1982) pushes its likely depositional age further back into the Calymmian period.

Cambrian sandstone (Bukalara Sandstone) and limestone (Top Springs Limestone) of the Georgina Basin blanket portions of the study area. These are generally only a veneer, not exceeding 100 m thickness, but the Bukalara Sandstone is up to 300 m thick in the Abner Range, in the south of the McArthur Basin study area.

Isolated outliers of Cretaceous conglomerate, sandstone, siltstone and mudstone, usually less than 20 m thick (Pietsch *et al* 1991), are scattered across much of the southern McArthur Basin. Cenozoic sediments also overlie much of the McArthur Basin study region, concealing large areas of Proterozoic section in the subsurface.

## Structure

Basement to the McArthur Basin was deformed, metamorphosed and subjected to significant felsic magmatism prior to ~1850 Ma, during the Barramundi Orogeny. The resulting structural framework controlled subsequent structural development (Rawlings 1999). Various fundamental basement influences have been identified, with northeast, north-northwest and northwest trends being the most common (Etheridge *et al* 1987, Etheridge and Wall 1994, Leaman 1998, Scott *et al* 2000). These have been repeatedly reactivated during the evolution of the McArthur Basin by a succession of extension, thermal subsidence and compression regimes.

North–south extension during Tawallah Group deposition was interrupted by an east–west compressional event in mid-Tawallah Group time (Bull and Rogers 1996). Overall regional flexure and strike-slip deformation, resulting from compressive stresses applied by orogenies at the southern edge of the North Australian Craton, subsequently continued, in the course of which the McArthur Group was deposited (Scott *et al* 2000). Extension causing block faulting was apparently superimposed on regional subsidence at the commencement of Barney Creek Formation deposition, resulting in NNW–SSE- and east–west-trending half-grabens to the west of the Emu Fault (Neudert and McGeough 1996), which may have been active as a transfer fault at this time. The McArthur Basin then experienced inversion, due to a northwest–southeast compressional event (Rogers 1996); this was possibly simultaneous with HYC mineralisation, which occurs towards the top of the Barney Creek Formation (Hinman *et al* 1994, Hinman 1996). North–south-trending depocentres then redeveloped (Neudert and McGeough 1996), creating accommodation space for subsequent sedimentation up to and including the Caranbirini Member. Relatively quiescent, dynamic long-wavelength and thermal subsidence then appears to have been the main influence on basin development, at least until Roper Group deposition. The final major structural event in the McArthur Basin was northeast–southwest-directed shortening, which affected all Proterozoic units, including the Roper Group (Rogers 1996). Apparent reactivations of north–south-trending faults affecting Cambrian units may be related to far-field effects of Australian Phanerozoic tectonic events, such as the Alice Springs Orogeny.

In spite of a long structural history, McArthur Basin strata are generally only gently folded with shallow dips. Some exceptions exist near faults, where bedding often steepens to 20–40°, and occasionally up to 70° (Pietsch *et al* 1991).

## Mineralisation

Stratiform sediment-hosted base metal (SSHBM) or ‘SEDEX’ deposits are characterised by single or multiple lenses of laminated or massive sphalerite and galena, which are usually accompanied by large amounts of pyrite, the Century deposit being a major exception. Each lens is of the order of several tens of metres thick (McGoldrick and Large 1998). Australian Proterozoic examples are hosted within carbonaceous shales and siltstones, but these host successions are interpreted to have been deposited in a range

of settings from shallow (<10 m) evaporitic lagoons (Lady Loretta; Dunster 1996) to deep (sub-photic zone), extensive (>20 km) water bodies (HYC; Oehler and Logan 1977, Large *et al* 2002).

All SSHBM deposits discovered in the Carpentaria Zinc Belt, thus far, have been situated on, or near major regional faults, but these have not necessarily been active during deposition of the ore host succession. Notwithstanding this, these faults have regularly been invoked in genetic models as conduits for mineralising hydrothermal fluid flow (eg McGoldrick and Large 1998, **Figure 4**).

The timing of base metal mineralisation with respect to its host sediments has been the subject of controversy for many decades, particularly at Mount Isa, the longest-known example. Reinterpretation of Mount Isa as a syngenetic-exhalative deposit from the initial hydrothermal replacement hypothesis was precipitated by discovery of the similar yet almost unmetamorphosed HYC deposit (Myers *et al* 1996). The opposing ‘syntectonic’ model proposes that the Mount Isa Zn-Pb ore is cogenetic with the Cu mineralised system, and that other Carpentaria Zinc Belt deposits may also be syntectonic (Perkins 1995, Laing *et al* 1990, Myers *et al* 1996). The genetic model most recently proposed for Century is in some ways intermediate between the syngenetic and syntectonic models, with ore minerals forming in the deep subsurface, associated with a hydrocarbon accumulation, during late diagenesis at the onset of basin inversion (Broadbent *et al* 1996). However, with some variations involving early diagenetic replacement (eg Hinman 1996 for HYC, McGoldrick *et al* 1996 for Lady Loretta), essentially syn-depositional mineralisation has remained the generally preferred model for most Carpentaria Zinc Belt SSHBM deposits, including Mount Isa.

Preference for the syn-depositional model is implicit in the following analysis, as it aims to reconstruct basin geometry at the time of deposition of the host succession. However, it remains pertinent to replacement scenarios, insofar as it indicates the distribution and thickness of carbonaceous (reducing) shales – the primary Zn-Pb ‘trap’ lithology.

## GEOLOGICAL DATASETS

The primary geological dataset employed was digitised from the BAUHINIA DOWNS mapsheet, produced by the Northern Territory Geological Survey (**Figure 3**, Pietsch *et al* 1991). The attribute structure for the digital geology polygons was developed from the scheme described by McClenaghan *et al* (1994). Attributes were populated mainly from the BAUHINIA DOWNS explanatory notes (Pietsch *et al* 1991), supplemented by other literature sources. Wherever possible, attribute codes were taken from existing Geoscience Australia (GA) authority tables.

Each stratigraphic unit present in the study area has been assigned a unique four-digit integer ID (CODE), based on its relative stratigraphic position. This number is the primary key linking the geology polygons to all their related attribute tables. Although stratigraphic relationships are specifically encoded in the polygon attribute scheme, the numbering system is also hierarchical with ID codes incremented according to their stratigraphic status; eg, individual

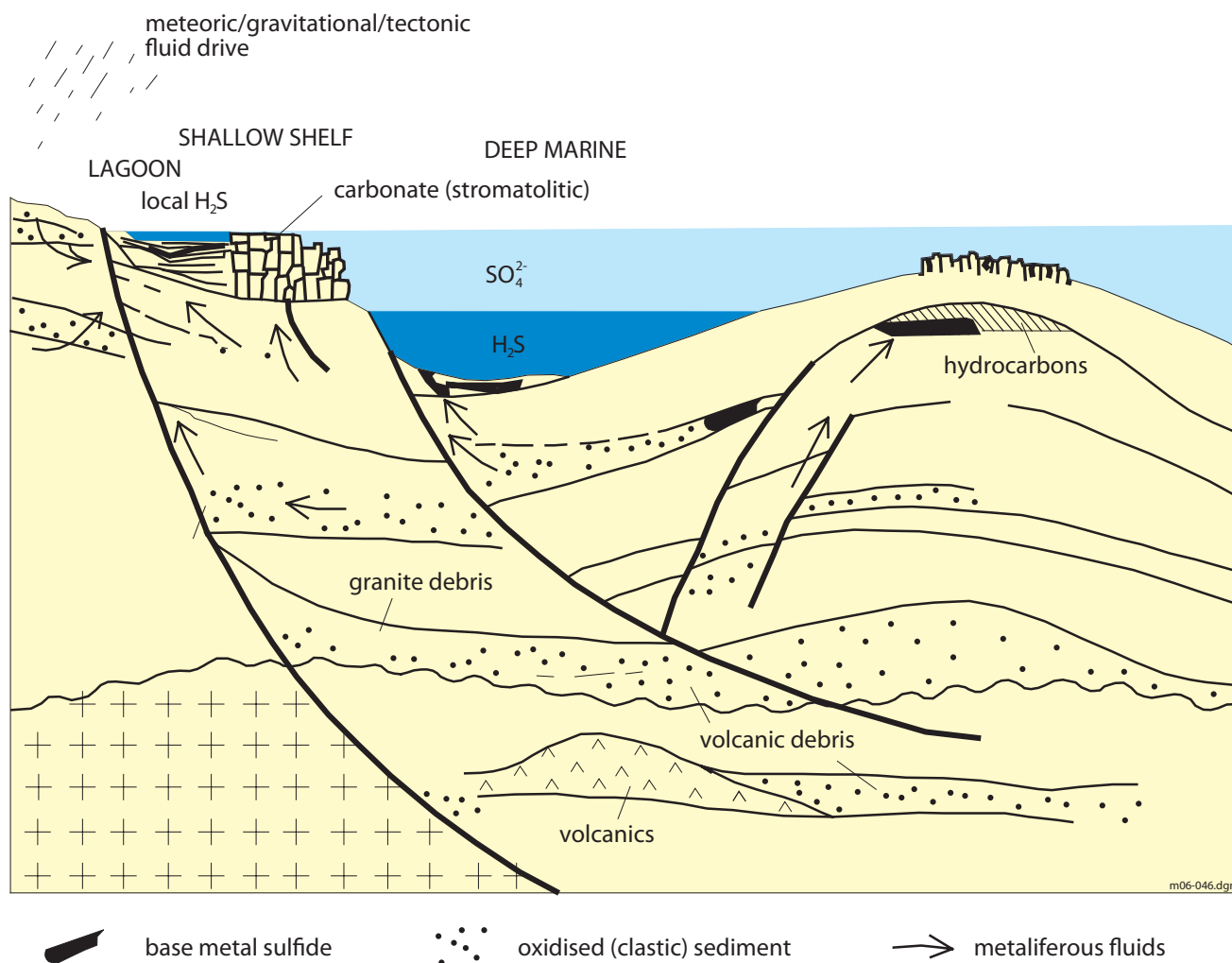


**Figure 4.** Schematic metallogenic scenarios for Proterozoic SSHBM deposits, after McGoldrick and Large (1998). Note the importance of sub-basins in localising potentially base metal-trapping reducing environments.

formations are given ID codes in increments of 10, while sub-groups increment in multiples of 100. Maintenance of this relationship greatly assists automatic legend production with map units appearing in their stratigraphic order, and facilitates polygon selection according to relative stratigraphic age, where this is not adequately defined by radiometric dating. For example, queries such as ‘select all Umbolooga Subgroup units older than the Teena Dolostone’ are possible using the stratigraphically-ordered hierarchical coding system, a set which could not be calculated directly from radiometric age constraints.

Stratigraphic information is encoded in the table STRAT.DAT. There is a many-to-one correspondence between the primary geology polygon coverage and this table, with the field CODE being common to both. A typical extract from STRAT.DAT is shown in Table 1. Descriptions of the most important fields for the purposes of this paper follow.

STRMIN and STRMAX are the minimum and maximum measured true thicknesses of the formation (in metres). Note that these dimensions are indicative only, being based on a limited number of measured sections and photo-interpretation, both within and outside the mapped region. A STRMIN equal to zero thus means that the unit is observed to lens out, but a STRMIN greater than zero does not

necessarily imply that the unit occurs throughout the basin.

LOCAL uses two-letter codes to denote geographic or descriptive geologic localities (eg ‘TR’ = ‘Tawallah Range’, ‘FI’ = ‘Foelsche Inlier’). Stratigraphic formations that vary systematically in thickness and/or composition between localities across the region have been given their own unique CODE, in order to retain this spatial variability. An example of a stratigraphic unit with multiple CODEs in Table 1 is the Mallapunyah Formation (Pml), which has codes ranging from 3710 to 3715, depending on locality, and correspondingly varying thickness attributes.

The lithological attribute table LITH.DAT (Table 2) has a many-to-many correspondence with the primary geological layer, linked by the unique geological map unit ID CODE. Each record in LITH.DAT represents a unique lithology present within the rock unit defined by CODE. A one-to-many relationship thus exists between the stratigraphic (STRAT.DAT) and lithological (LITH.DAT) attribute tables through the CODE item. Selection of a given stratigraphic unit, for example the Wollogorang Formation (CODE = 4040) will retrieve all lithological attribute records with the corresponding CODE. This relationship also works in reverse; thus, selection of all lithologies containing pyrite (MIN = ‘PY’) will retrieve all stratigraphic units satisfying



CODE	SYMBOL	LOCAL	GRP	SBGRP	FRM	MBR	MIN AGE	MAX AGE	STR MIN	STR MAX
3600	Em		McArthur	Umbolooga			1600	1719	2000	3300
3610	Emx		McArthur	Umbolooga	Reward Dolomite		1600	1647	30	350
3620	Emq		McArthur	Umbolooga	Barney Ck Fm		1633	1647	10	900
3630	Emp		McArthur	Umbolooga	Teena Dolomite		1633	1719	15	130
3632	Empc		McArthur	Umbolooga	Teena Dolomite	Coxco Dolomite	1633	1719	15	70
3640	Eme		McArthur	Umbolooga	Emmerugga Dolomite		1633	1719		620
3642	Emei		McArthur	Umbolooga	Emmerugga Dolomite	Mitchell Yard Dolomite	1633	1719		
3644	Emea		McArthur	Umbolooga	Emmerugga Dolomite	Mara Dolomite	1633	1719		
3650	Emf		McArthur	Umbolooga	Myrtle Shale		1633	1719	40	60
3660	Emi		McArthur	Umbolooga	Leila Sandstone		1633	1719	0	30
3670	Emt		McArthur	Umbolooga	Tooganinie Fm		1633	1719		200
3680	Emd		McArthur	Umbolooga	Tatoola Sandstone		1633	1719	80	350
3681	Emd	TP	McArthur	Umbolooga	Tatoola Sandstone		1633	1719	80	150
3690	Ema		McArthur	Umbolooga	Amelia Dolomite		1633	1719	50	150
3691	Ema	SB	McArthur	Umbolooga	Amelia Dolomite		1633	1719	150	180
3710	Eml		McArthur	Umbolooga	Mallapunyah Fm		1633	1719	100	450
3711	Eml	MD	McArthur	Umbolooga	Mallapunyah Fm		1633	1719	200	220
3712	Eml	TR	McArthur	Umbolooga	Mallapunyah Fm		1633	1719	200	220
3713	Eml	MH	McArthur	Umbolooga	Mallapunyah Fm		1633	1719	100	110
3714	Eml	FI	McArthur	Umbolooga	Mallapunyah Fm		1633	1719	250	300
3715	Eml	WB	McArthur	Umbolooga	Mallapunyah Fm		1633	1719	300	450

**Table 1.** Extract from the stratigraphic data table STRAT.DAT.

this criteria, even though not all lithologies for those CODES actually contain pyrite.

Lithological attributes are constructed hierarchically after McClenaghan *et al* (1994), in order to facilitate queries on as many levels as possible. Encoded levels of lithological classification range from detailed (for example, sedimentary structures in TEXT) to very basic (igneous/sedimentary/metamorphic categorisations in CLASS). These and other attribute fields in LITH.DAT are discussed more fully below. Although this scheme makes the overall attribute database somewhat larger than is strictly necessary, this slight disadvantage is far outweighed by gains in the simplicity of queries. A request to select all sedimentary rocks, for example, might otherwise have to be constructed by the selection of all possible sedimentary lithologies, with all the extra effort

and possibility of error or omission that such a query would entail.

All entries in the extract from LITH.DAT (**Table 2**) relate to codes in GA authority tables (<http://www.ga.gov.au/oracle/lookups/lookups.php>), adapted to the structure of this GIS. The fundamental classification of lithologies involves one compositional and two genetic orders of categorisation. The items CLASS and TYPE are together roughly equivalent to the ROCK\_TYPE codes described in GA's field notebook guide (Blewett 1993). CLASS is a single-character text field containing the simplest genetic lithological divisions (Igneous, Metamorphic, Sedimentary, Unconsolidated), which are in turn subdivided by the TYPE item (three- or four-character codes), essentially on a more detailed genetic basis. Virtually all sedimentary rocks in the McArthur Basin classify as being of clastic (EPC) or chemical (CHEM)

CODE	LITH_ID	CLASS	TYPE	COMP	LITH	PROP	TEXT	MIN
4040	357	S	CHEM	CARB	DLST	20	F TN SUL BTM	PY
4040	358	S	CHEM	CARB	DLST	5	F STRO SUL BTM	PY
4040	359	S	EPC	CARB	BX	1	C DMT	
4040	360	S	EPC		SHLE	15	EVPT PS	
4040	361	S	EPC		SHLE	15	ORG SUL DMT	PY
4040	362	S	EPC		SDST	15	FER DMT XB	
4040	363	S	EPC	QZ	ARNT	20	WH	
4040	364	S	EPC		CNGL	5	PB	
4040	365	S	CHEM	CARB	DLST	5	XL	
4050	366	I	EXV	MAF	BLT	30	RE BR GY F M	
4050	367	I	EXV	FLS	RHY	10	AB BA	
4050	368	S	EPC		SHLE	15	HFL	
4050	369	S	CHEM	CARB	DLST	10	F SLY HFL	
4050	370	S	EPC		SDST	5	FER	
4050	371	S	EPC	CARB	BX	5	DMT	
4050	372	I	ITV	MAF	DLT	25	HK MTS	

**Table 2.** Extract from lithological data table LITH.DAT.



origin. Mixtures of the two are handled using qualifiers; thus a silty dolostone is categorised as being of CHEM type, but will contain SLY (for silty) in the TEXT field.

COMP describes the dominant composition of the lithology. Minor constituents or mixed compositions are encoded using the TEXT qualifiers, though following GA's usage some exceptions have been made, eg QF for 'quartzo-feldspathic' as well as QZ (quartzose) and FEL (feldspathic).

The LITH field explicitly characterises the lithology in terms of codes from the GA LITHOLOGIES authority table. A convention of four-character codes for sedimentary lithologies and three-character codes for igneous and metamorphic lithologies is generally followed. Most defined lithologies are taken directly from Pietsch *et al* (1991), supplemented by Jackson *et al* (1987) who used a basic grainsize terminology for the classification of carbonate rocks, such as dololite and dolarenite. These terms were not supported by LITHOLOGIES at the time of compilation, and were adapted for this GIS by use of the relevant qualifiers on the general rock name DLST (for dolostone); thus a dololite is coded in LITH as DLST, with F (for 'fine-grained') in the TEXT field.

The PROP item, for 'proportion', is an integer field giving an indication of the volumetric proportion of the particular lithology, expressed as a percentage of the total stratigraphic unit. These have been estimated from text descriptions, as well as published measured stratigraphic sections in Pietsch *et al* (1991) and Jackson *et al* (1987). As such, they are strictly a qualitative indication only, particularly because of the likelihood of lateral variations within stratigraphic units away from measured sections.

The TEXT field contains qualifiers that enable a full description of a given lithology, by modifying or augmenting the coarser classifications of the other fields. The qualifiers may be of any type, indicating compositional, grainsize, internal structural, sorting and other features. These range from basic descriptors like P or W for 'poorly-sorted' and 'well-sorted', through to more exotic designations like SUL for 'sulfidic' or LTX for 'low-angle trough cross bedding'.

Unusual or diagnostic minerals appear in the MIN ('mineralogy') field. There may be some overlap between this field and TEXT, thus PY (pyrite) may appear in MIN in addition to PYR (pyritic) or SUL (sulfidic) in TEXT. MIN entries for many lithologies may actually refer to pseudomorphs of the given mineral (usually GP for 'gypsum' or HL for 'halite'), but these have been retained for their diagnostic value.

A mineral occurrence database was also incorporated in the GIS, adapted from NTGS' MINLOC database. An extract is shown in Table 3. Host unit and lithology information are included by links to the STRAT.DAT and LITH.DAT tables through the HOST and HOSTLITH\_ID fields, respectively.

### Geophysically-derived datasets

It is far more useful, in terms of geological import and metallogenic analysis, to bring the tools of GIS to bear on structures and surfaces interpreted from the geophysical data, rather than on the data itself. The geophysical component of the McArthur Basin GIS is composed of interpretations by Leaman (1998 and associated references) from gravity, magnetic and seismic data of the most volumetrically significant units in the basin. An account of the interpretation methodology is given in Leaman (1994, 1996, 1997).

Geophysical interpretation layers were constructed by digitising interpretive contour plots produced for various McArthur Basin sub-regions (D Leaman, pers comm) and compiling them for the entire basin, including the main BAUHINIA DOWNS study area. The source data used in the GIS is thus somewhat more detailed than that appearing in Leaman (1998). Each contoured surface (either structure contours or isochores) has been built as a Triangulated Irregular Network (TIN), then transformed into a raster, using quintic interpolation. Every cell in the resulting grid thus has a value representing either depth-to-interface or unit thickness, measured in metres. Zero or small negative values arising from gridding artifacts were converted to null values.

This gridding process enables 3-D visualisation and surface analysis of the structure contours or isochores

MINDEP-ID	NAME	MAJCOM	MINCOM	OPS	SHAPE	HOST	HOSTLITH_ID	OREMIN1
25	Biondi	Pb		P	SB	3610	188	GN
26	Emu Plains	Pb Zn	Ag	P	SF	3620	195	SP
27	Bamey Creek	Pb	Ag	O	SF	3642	216	GN
28	Bameys	Pb	Ag	O	SF	3630	202	GN
29	HYC	Zn Pb Ag	Cu	OM	SF	3620	195	SP GN
30	Cooley II	Cu	Pb Zn	D	SB	3640	212	CCP
31	Cooley I	Zn Pb	Cu	D	SB	3640	212	GN
32	Cooley III	Pb Zn	Cu	D	SB	3640	212	GN SP
33	Ridge I	Pb Zn	Cu	D	SB	3620	198	GN SP
34	Ridge II	Pb Zn	Cu	D	SB	3620	198	GN
35	Buffalo Lagoon	Pb		O	SB	3642	216	GN
36		Ba		O	VN	4050	366	BRT
37	Mitchell Yard	Zn Pb		P	SF	3620	195	SP
38	Myrtle Basin	Pb Zn	Ag Cu	P	SF	3620	195	SP
39	Cooks	Zn Pb		D	SB	3610	191	GN SP
40	Cox	Zn Pb		D	SB	3610	191	SP GN

**Table 3.** Extract from mineral occurrence database. 'MAJCOM' = major commodity, 'MINCOM' = minor commodity, 'OPS' = status (Occurrence, Prospect, Deposit, Operating Mine). In SHAPE, 'SB' = stratabound, 'SF' = stratiform, 'VN' = vein. Mineral codes in OREMIN1 are from the GA Mineral Names lookup table (<http://www.ga.gov.au/oracle/lookups/lookups.php>).

defined by the potential field interpretation. These grids can then be overlain by any of the other datasets contained in the GIS, for the purpose of elucidating relationships between deep, fundamental basin structures and the observed surface geology and mineral occurrence distribution. Examples are shown in Duffett and Leaman (1997).

The original interpretation was of coarse resolution; isochores and structure contours being at spacings ranging from 100 m to 5 km vertically, with an uncertainty of similar magnitude in horizontal location. This is partly due to the sparseness of the original potential field data (gravity generally of 11 km spacing, aeromagnetic flight lines generally 1500 m apart), and partly due to the primary objectives of the original interpretation, which were to convey the style and shape, and gross volume of basin forms, rather than to provide precise estimates of their three-dimensional location.

Consequently, there is a danger of over-enlarging and over-interpreting this material. However, there are a number of advantages to this method of presenting geophysically-derived information. All the tools commonly used to enhance the visualisation of primary geophysical data can be applied to rasters that carry much more ‘value-added’ geological information than the raw gravity and magnetic data. Grid analysis can also be used to generate derived surfaces, for

example, the distribution of ‘background’ (not explicitly defined by potential field modelling) material produced by subtraction of two other grids representing disposition of stratigraphically adjacent basin components. One significant limitation is the 2.5D nature of the grid analysis tools used, in that for each surface, only one z can be defined for any given x,y coordinate.

Five structural surfaces were constructed, covering the entire southern McArthur Basin region. From the lowest (generally) unit upwards, these are: depth to basement granite; depth to base of magnetic felsic rocks (a pre-Tawallah Group igneous accumulation of uncertain affinity, possibly containing a significant mafic component; see Leaman 1996, 1998); thickness of felsic rocks; base of mafic volcanic rocks; and thickness of mafic volcanic rocks.

Other surfaces were produced that are restricted to the main BAUHINIA DOWNS GIS study area, and represent units higher in the basin stratigraphy than the major igneous accumulations described above. These include grids of thickness and depth-to-top (structure contours) of upper Tawallah Group mafic volcanic rocks and also, the thickness of more massive (in terms of density) McArthur Group carbonate-dominated units. Only the last of these was employed directly in the analysis described by this paper (Figure 5). Other metallogenic applications utilising all the

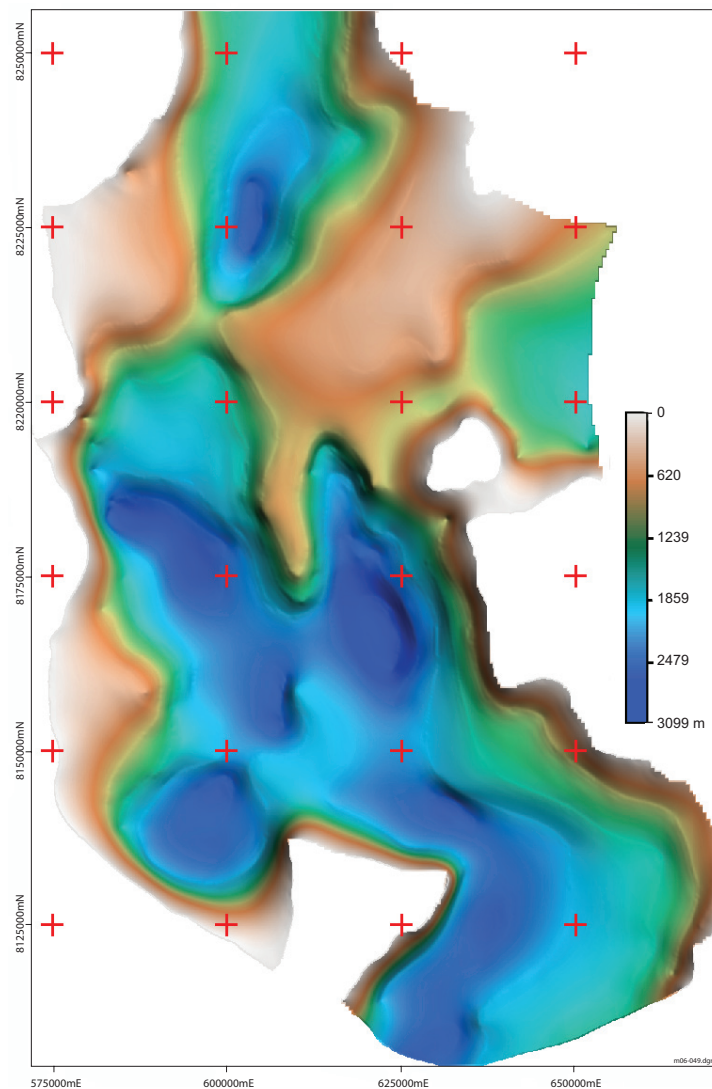


**Figure 5.** Presently preserved thickness of carbonate-dominated McArthur Group, interpreted from geophysical data. See text for details.

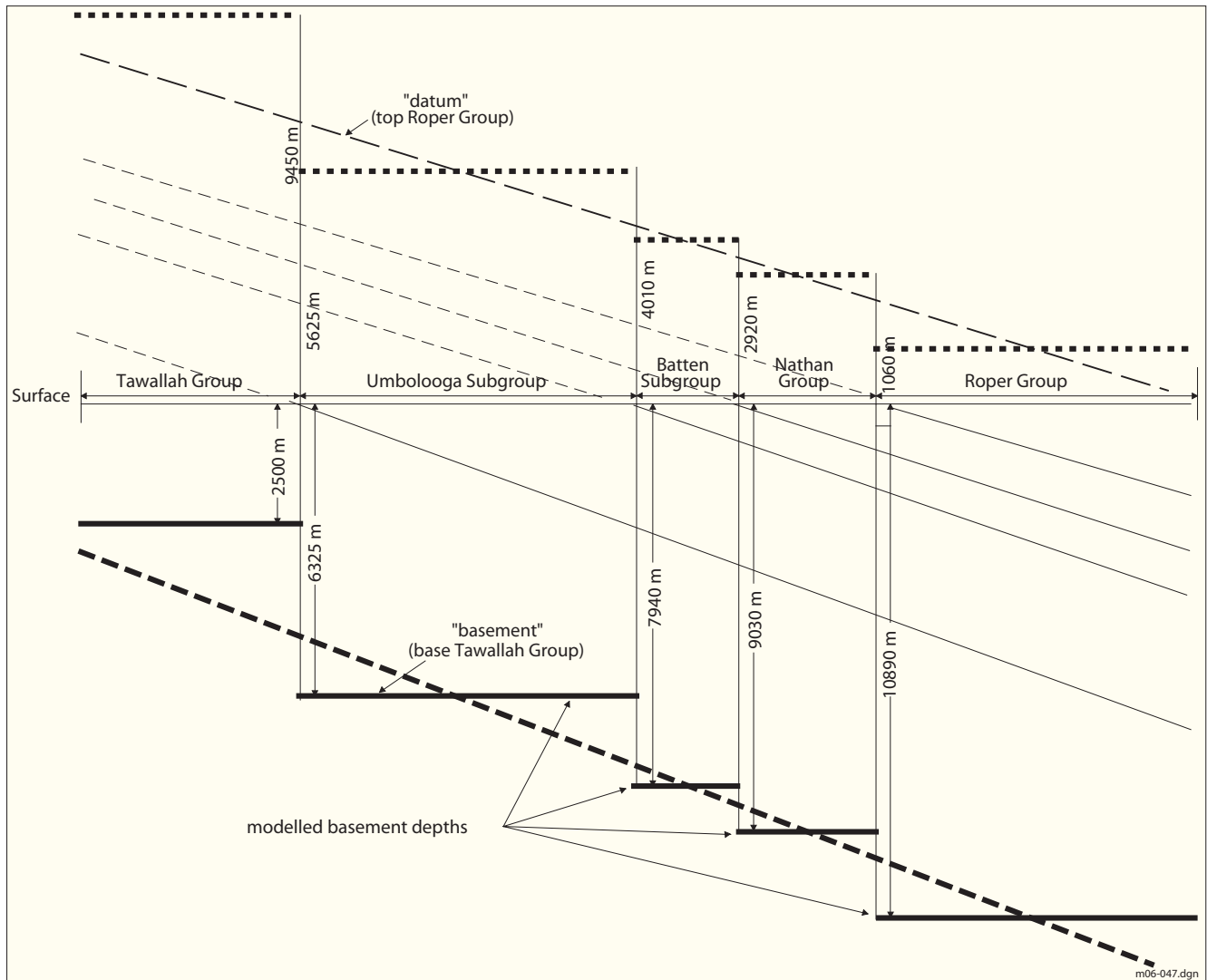


**Figure 6.** Schematic diagram using a simplified example to demonstrate how basement (or any other basin stratigraphic horizon) depth may be modelled from outcrop geology using thickness attributes in a GIS. See text for details.

interpretive basin architecture datasets were described in Duffett (2000).

## ANALYSIS

### Geological attribute-based basin visualisation

An initial 3-D picture of the basin, relying solely on surface geological data and measured stratigraphic thicknesses, was

developed by generation of coverages, comprising ‘predicted’ structure contour values for any given stratigraphic unit. The method (Figure 6) is based on a stratigraphic attribute table (eg Table 4) keyed to the geological map coverage. Representative stratigraphic thicknesses were derived for each unit by calculating the mean of all values measured (mainly sourced from Pietsch *et al* 1991) in the study region. In many cases, this was simply the midpoint between the quoted minimum and maximum stratigraphic thicknesses.

Unit	STRMED (thickness in m)	ZMEAN (av elevation wrt datum)	Implied basement depth ( $z_{\text{mean unit}} - z_{\text{mean basement}}$ )
Roper Group	2120	-1060	10890
Nathan Group	1600	-2920	9030
Batten Subgroup	580	-4010	7940
Umbolooga Subgroup	2650	-5625	6325
Tawallah Group	5000	-9450	2500
basement (base Tawallah)		-11950	0

**Table 4.** Simplified example of STRAT.DAT consolidated to group/subgroup level, showing thickness attributes used to construct Figure 6.

The results were entered into the field STRMED, with some additional records and stratigraphic codes created to handle gross regional changes in measured thickness in some units. A datum surface was defined at the top of the Proterozoic McArthur Basin succession, ie, the top of the Roper Group, and the STRMED value converted to a number (ZMEAN), representing the stratigraphic distance, in metres, from this datum surface. ZMEAN for any given unit  $i$  is essentially given by the total thickness of overlying units plus half the thickness of the unit  $i$ , multiplied by  $-1$  to express elevation with respect to the datum at the top of the Roper Group; or, algebraically:

$$ZMEAN = -1 * \left( \sum_{i=1}^{i-1} STRMED_i + STRMED_i / 2 \right)$$

These values represent elevation with respect to this datum surface and thus are negative, decreasing with

stratigraphic age. Each Proterozoic geology polygon was thus attributed (via the link to STRAT.DAT) with a value representing the elevation of the outcropping unit within the basin stratigraphic succession. These values range from  $-133$  in the case of the McMinn Formation at the top of the Roper Group, down to  $-12560$  for the Yiyintyi Sandstone at the base of the Tawallah Group.

The geological data were thus used to directly infer present basin geometry, by making the simplifying assumption of 'layer-cake' stratigraphy (Figure 6). The resulting maps (eg Figure 7) provide a quantitative visualisation of basin structure, not obvious on casual inspection of the standard geological map, and particularly emphasise the magnitude of vertical displacement across faults. The Tawallah Fault is especially prominent in these terms (Figure 7), as is the Abner Fault, which is evidently a continuation of the Tawallah Fault on the western edge of the Abner Range,

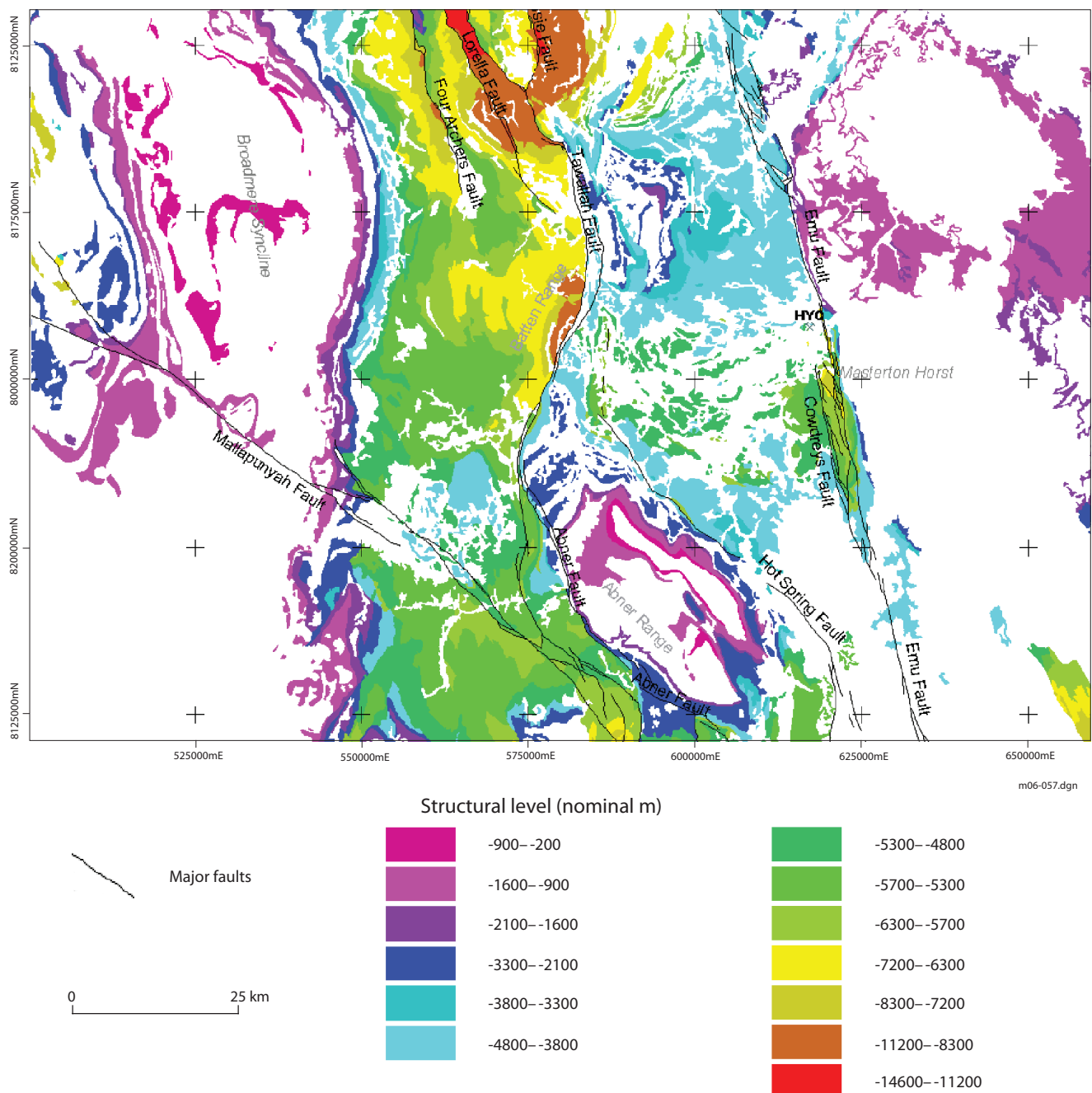


**Figure 7.** Structural level exposure map. Warm colours indicate structurally uplifted areas. See text for details.



albeit at a higher level in the stratigraphy (cooler colours in [Figure 7](#)). The Emu Fault is of rather enigmatic character, with little apparent displacement across its northern and southern ends in [Figure 7](#), but major deformation in the vicinity of the fault within 25 km of the HYC deposit. The structurally anomalous character of the Tawallah Group inlier adjacent to the Emu Fault (Masterton Horst) is especially conspicuous. The predominantly strike-slip character of the Mallapunyah Fault is clearly apparent. A feature with quite striking apparent vertical displacement is the fault splaying northeastwards from the Emu Fault from around 8200000mN. A major reason for this is the absence of the Nathan Group, as well as faulting. The magnitude of regional folds is also

prominently displayed, the north–south-trending Broadmere Syncline and the syncline at Abner Range, both of which have upper Roper Group in their cores, being examples. More subtle, but nonetheless potentially significant, is intra-McArthur Group uplift in the region southwest of HYC (see also [Figure 8](#)), which appears to have an east–west-trending aspect. The gross structure implied is similar to an anticlinal box fold, with a wavelength around 15 km. In dimensions, it appears to be similar to the uplift represented by the Batten Range on the adjacent western side of the Tawallah Fault and may have a common origin.

[Figure 7](#) and other maps such as [Figure 8](#), made possible by the stratigraphic thickness data structure

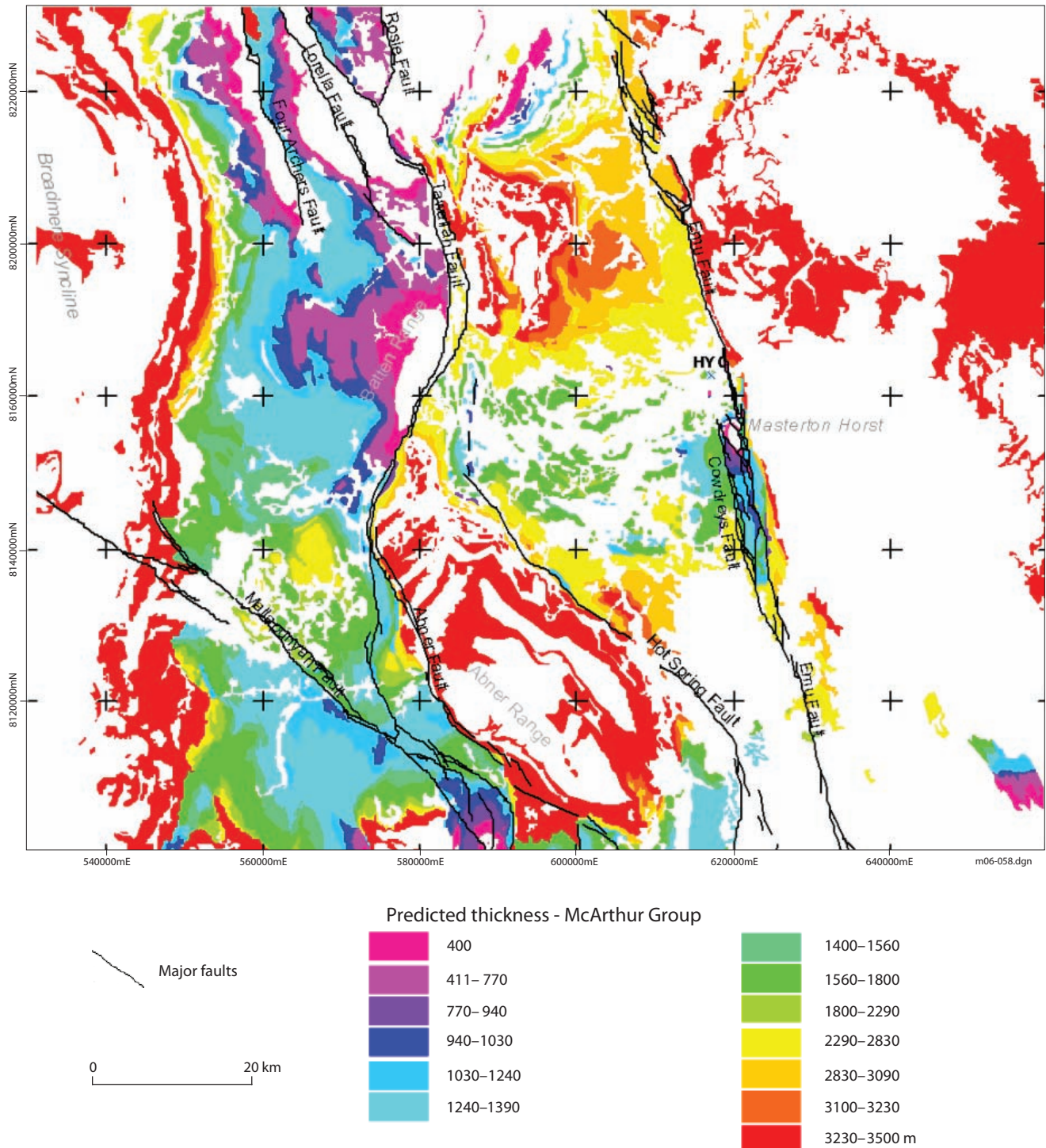


**Figure 8.** Present McArthur Group thickness, inferred from outcrop geology and stratigraphic thickness attributes. See text for details.

described (which might be termed *stratigraphic topology*), effectively make explicit the knowledge of depth extent implied by the stratigraphic column. The depth of an underlying unit or contact may be predicted from surface geology and the attribute table; eg, the base of the McArthur Group (base Masterton Sandstone), from which McArthur Group thickness in **Figure 8** was derived. This enables ‘actual’ three-dimensional basin architecture inferred from geophysical data to be analysed in terms of its anomalous character with respect to surface geology (see below; **Figures 13a and b**).

There are some obvious limitations to this approach. The same stratigraphic level is applied to the entire extent of each geology polygon, with no distinction between areas of the polygon near upper or lower stratigraphic contacts (**Figure 6**). This results in mis-estimation of the depth of underlying units by up to  $\frac{1}{2}a \tan \theta$ , where  $a$  is the apparent thickness of the surface unit and  $\theta$  is dip, in the worst-case situations at the upper and lower contacts of the exposed unit. The relative magnitude of this error diminishes with increasing stratigraphic distance between the surface unit and the horizon of interest, and is largely negligible where the mapped stratigraphic resolution is sufficiently high.

Depth of underlying units is additionally underestimated by a factor of  $1 / \cos \theta$ , being the difference between the true stratigraphic thicknesses modelled and vertical thickness. However, dips exceeding  $25^\circ$  (equating to a thickness underestimation of about 10%) are comparatively rare in the region of the McArthur Basin studied, being generally restricted to zones adjacent to major faults. These geometric errors are not considered unduly significant in the semi-quantitative context of subsequent analysis and interpretation.

Another drawback is that stratigraphic levels cannot be derived for areas obscured by thin Cenozoic cover, limiting the extent to which comparisons can be made with interpretations of underlying broad structure.

All of these objections could be addressed to some extent in further work by attaching the stratigraphic level attribute to bounding arcs as well as to polygons, incorporation of dip and strike data, and use of airborne EM or high-resolution magnetic data to infer Proterozoic geology beneath thin cover. The former two refinements might be implemented by interpolation of geology polygons and arcs, incorporating dip and strike information, to a grid data structure. Conversion to raster is a step required in any case, to enable direct comparison and analysis with respect to the geophysically derived structural surfaces.

### Automatic unconformity detection

Intra-basinal unconformities denote areas that have been elevated with respect to the contemporaneous basin, resulting in erosion or lack of deposition. As such, their spatial and stratigraphic distribution effectively maps both the location and timing of intra-basinal uplifts and, by omission, possible sub-basin locations.

A technique for automatic extraction of unconformities from detailed geological maps was developed utilising the topological data structure of Arc/Info and two attribute fields added to the stratigraphic look-up table STRAT.DAT. For

each record (representing a stratigraphic unit) in the look-up table, these fields (UNDER and OVER) contain the unique code for the stratigraphic unit, which would, in a complete basin succession, conformably underlie and overlie the unit described by the record (**Table 5**).

These stratigraphic polygon attributes were attached to their bounding arcs by hard links based on internal arc record numbers identifying the polygons on the left and right side of the arcs (LPOLY# and RPOLY#). Following queries to eliminate faults and arcs representing nonconformable Proterozoic/Phanerozoic contacts, the stratigraphic unit on the left side of each non-fault arc bounding a Proterozoic geological polygon was identified using the LPOLY# item. The polygons on the right side of the selected arcs were then queried through the RPOLY# item. If the result did not match the ‘expected’ geologic entity code, corresponding to the units conformably above or below the unit originally identified on the left side of the polygon, the arc was identified as an unconformity, and tagged as such in the arc attribute table. The UNDER and OVER attributes were utilised to designate the unconformity as one of four types: intra-group (where both the underlying and overlying units belong to the same stratigraphic group); ‘expected’ inter-group (where an unconformity is present by definition, but both the topmost underlying formation/member and the basal overlying formation/member of the respective groups are present); inter-group 1 (where one or more of either the topmost underlying or basal overlying units is missing at the unconformity surface); and inter-group 2 (where an entire group is absent).

This method was extended to calculate the ‘magnitude’ of the unconformity, by reference to the stratigraphic thickness attributes described above. Using the absolute stratigraphic level described by ZMEAN, the total measured thicknesses (obviously measured elsewhere in the basin) of ‘missing’ units (stratigraphically between the polygons on either side of the arc) were used to determine the amount of missing sedimentary section, in metres. This figure was also calculated to the arc attribute table. The link via the left- and right-polygon codes to the stratigraphic attribute table also identifies the stratigraphic time interval represented by the unconformity.

CODE	UNIT	UNDER	OVER
3610	Reward Dolomite	3620	3346
3620	Barney Creek Formation	3632	3610
3630	Teena Dolomite	3640	3632
3632	Coxco Dolomite Member	3630	3620
3640	Emmerugga Dolomite	3650	3630
3642	Mitchell Yard Dolomite Member	3644	3630
3644	Mara Dolomite Member	3650	3642
3650	Myrtle Shale	3660	3644
3660	Leila Sandstone	3670	3650
3670	Tooganinie Formation	3680	3660

**Table 5.** Extract from appended stratigraphic data table. The CODE field contains the identification number unique to each stratigraphic unit in the study area, to which the ‘stratigraphic topological’ attributes UNDER and OVER also refer.

The resulting arc attribute data were extracted into unconformity attribute tables for further analysis (Figures 10, 11, 12). These tables relate the standard GIS line attributes, such as length, through a unique ID and the stratigraphic attribute table, to the unconformity attributes

of type, stratigraphic position (defined by both underlying and overlying unit) and thickness of missing sediment.

The unconformity maps that can be generated as a result of this process (eg Figure 9) indicate areas of uplift or low subsidence during basin development, where stratigraphic

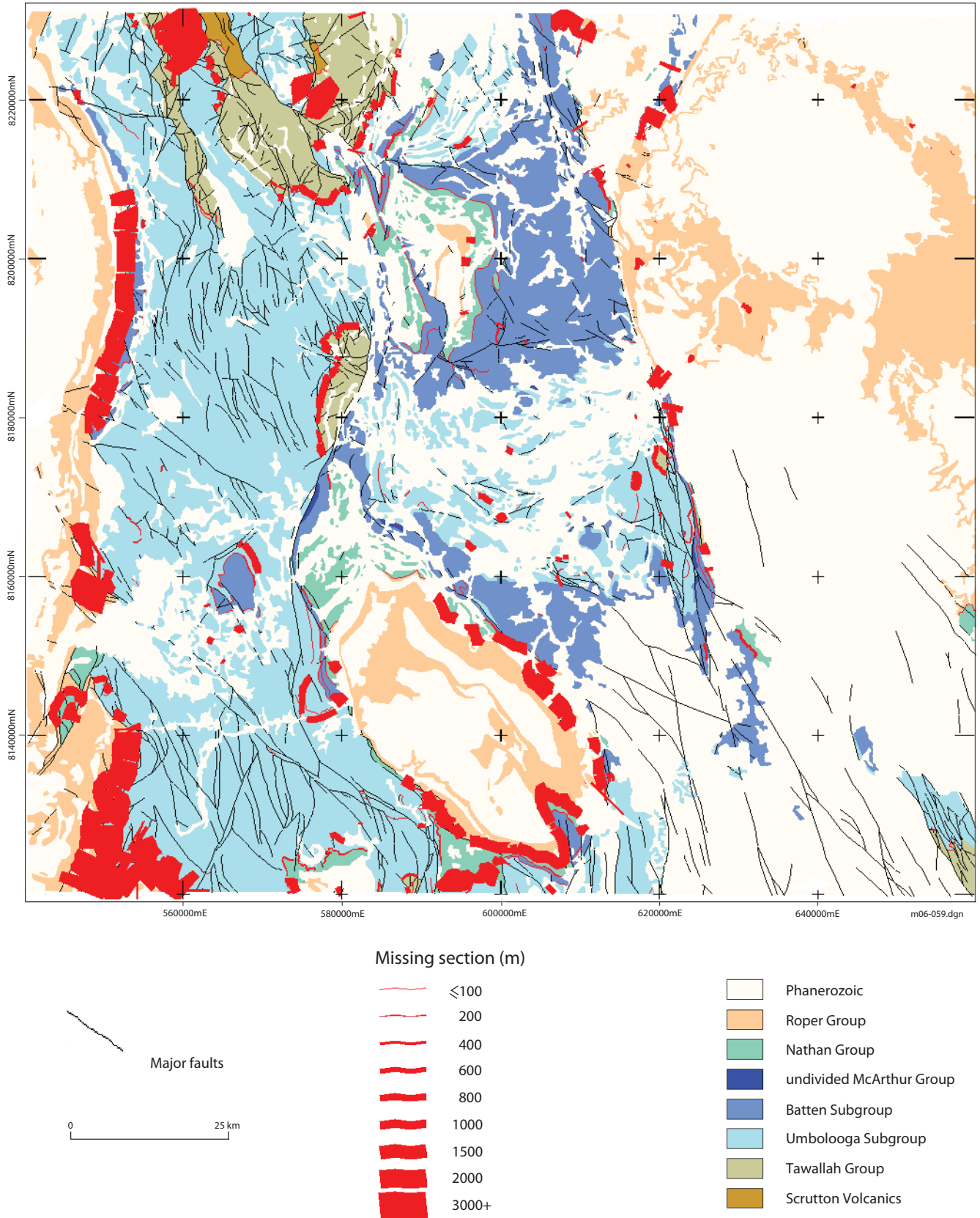


**Figure 9.** Central McArthur Basin unconformity map, showing amount of section missing at mapped horizons (in terms of nominal thickness of absent units) from a notional complete stratigraphic column. See text for details.



units are absent, due to erosion, lack of deposition, or both. The unconformity magnitude can be interpreted as indicating the magnitude and persistence of these locally elevated regions within the basin, which can act as focusing structures or drivers of basinal fluid flow. Importantly, the unconformities mapped can be queried on the basis of the relative age of their overlying or underlying units, so that the distribution of unconformities within certain intervals may be examined.

The most prominent unconformities (where the greatest thicknesses of a notional complete section are absent) invariably comprise contacts between stratigraphic entities at the group level (Figure 10). The frequent absence of the Tanumbirini Rhyolite, Warramana Sandstone and Gold Creek Volcanics from the top of the Tawallah Group accounts for the identification of several hundred metres of missing section at the Tawallah–McArthur Group contact in many areas (Figures 9, 12). This observation is consistent with deposition of the upper Tawallah Group in a syn-rift setting. The largest absence of section is observed in the section dipping west and north away from the Tawallah Group inlier in the Batten Range. This supports the proposition based on

palaeocurrent and structural data (Bull and Rogers 1996) that the Batten Range region was elevated during later Tawallah Group time. Generally, there are a few hundred metres of section missing at all top-Tawallah Group contacts west of the Emu Fault, including the Masterton Horst near HYC and Mallapunyah Dome. Notable exceptions are a small section (12 km long) around 562000mE 8212000mN (near several base metal prospects, including Great Scott and Johnstons) and the Foelsche Inlier area, where no, or minor hiatuses are identified. These may denote late Tawallah Group time sub-basins or otherwise relatively depressed areas enabling preservation of a near-complete Tawallah Group succession.

There are a number of intra-Umbolooga Subgroup unconformities detected, suggesting a reasonable level of structural activity during this phase of basin development. Many of these unconformities (probably disconformities) occur within a strip oriented east-northeast, extending from the Mallapunyah Fault near 560000mE 8160000mN to the Emu Fault immediately south of HYC. Many ‘unconformities’ are associated with the absence of either the Teena Dolostone or its subordinate Coxco Dolostone

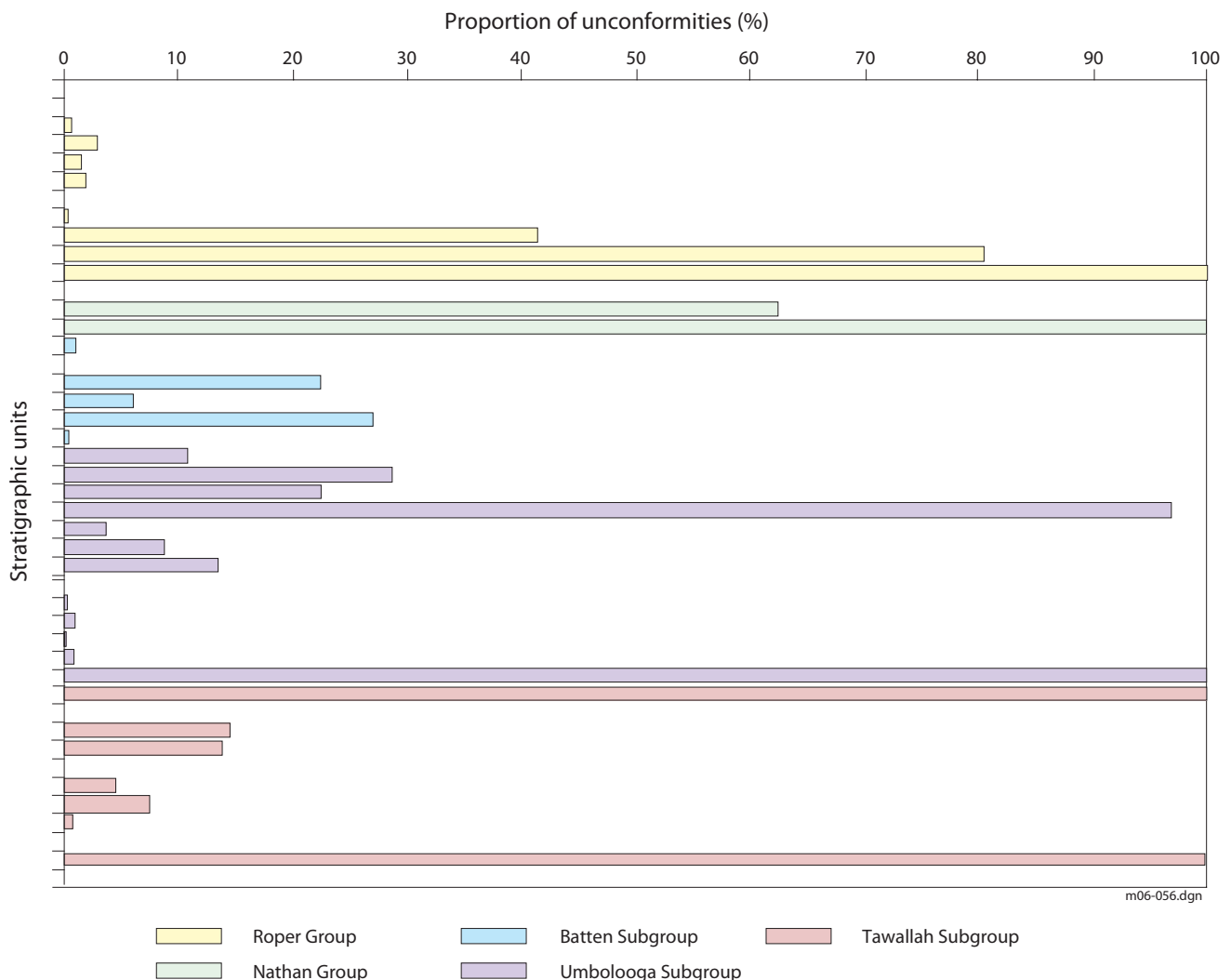


**Figure 10.** Distribution of unconformable surfaces in the stratigraphic column, based on the unconformity attribute data generated within the GIS. Each bar in the chart corresponds to the lower contact of an individual stratigraphic unit (formation or member), and the length of each bar indicates the proportion of these contacts that are unconformable surfaces. The location of an unconformity within the column is defined by the overlying unit.



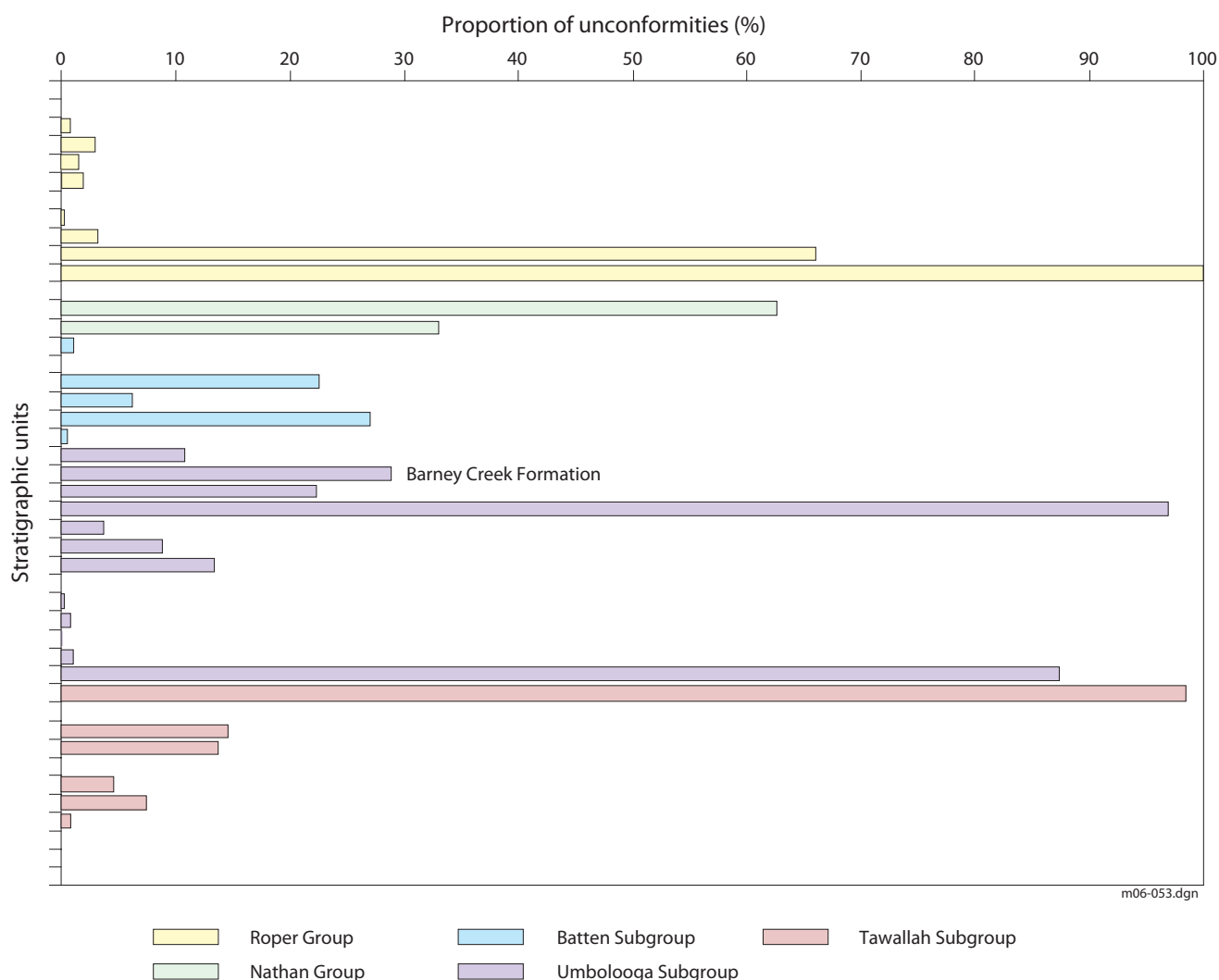


**Figure 11.** Distribution of unconformable surfaces in the stratigraphic column, constructed as in [Figure 10](#), but with ‘expected’ unconformities between complete sections of stratigraphic groups removed. The bar denoting the base of the Barney Creek Formation, host unit of the HYC deposit, is labelled for reference.

Member. As these units are differentiated substantially on the basis of diagenetic features, interpretations of these contacts as unconformities in the classic sense must be treated with caution. Other unconformities identified in [Figures 9](#) and [11](#) appear more genuine, and may be mapping a zone of irregular, discontinuous uplifts in the vicinity of the east-northeast-oriented strip, referred to above, active in middle to later Umbolooga Subgroup time. This phase of activity seems to have been more persistent west of the Tawallah Fault, where there are a number of points at which a small amount of section (usually either the Barney Creek Formation or Reward Dolostone) is missing. East of the Tawallah Fault, little erosion appears to have taken place near the Umbolooga–Batten Subgroup boundary, though some unconformities may be obscured by the generally more extensive Cenozoic cover in this region.

The anomalous intra-basinal structural activity characterising the upper Umbolooga Subgroup appears to have waned during Batten Subgroup time, with few unconformities detected.

The Nathan Group marks a substantial shift in regional deposition patterns, which largely accounts for the substantial unconformity defined at its base (the Nathan Group actually rests directly on the Tawallah Group in the

Tanumbirini Inlier in the west of the study area, with the entire McArthur Group missing). However, instability in sedimentation patterns appears to have persisted well into Nathan Group time ([Figures 9](#), [11](#) and [12](#)), and it may be that significant topographically driven fluid flow also took place at this time.

The most significant intra-Proterozoic tectonic event recorded by the automatic unconformity detection method took place in the interval between the Nathan Group and the time recorded by the base of the Roper Group. Queries of the stratigraphic attribute table indicate that the basal units of the Roper Group (Limmen Sandstone and Mantungula Formation) incise as deep as the Tawallah Sandstone, well down in the McArthur Group. The magnitude of sediment removed at this interval may be seen in [Figure 12](#). [Figure 9](#) indicates that this sediment removal took place mostly on the western side of the Batten Fault Zone, and reached a maximum in the southwestern corner of the study area.

### Basin reconstruction

Knowledge of the basin shape contemporaneous with mineralisation is critical for understanding of the palaeohydrogeological factors resulting in the focusing of

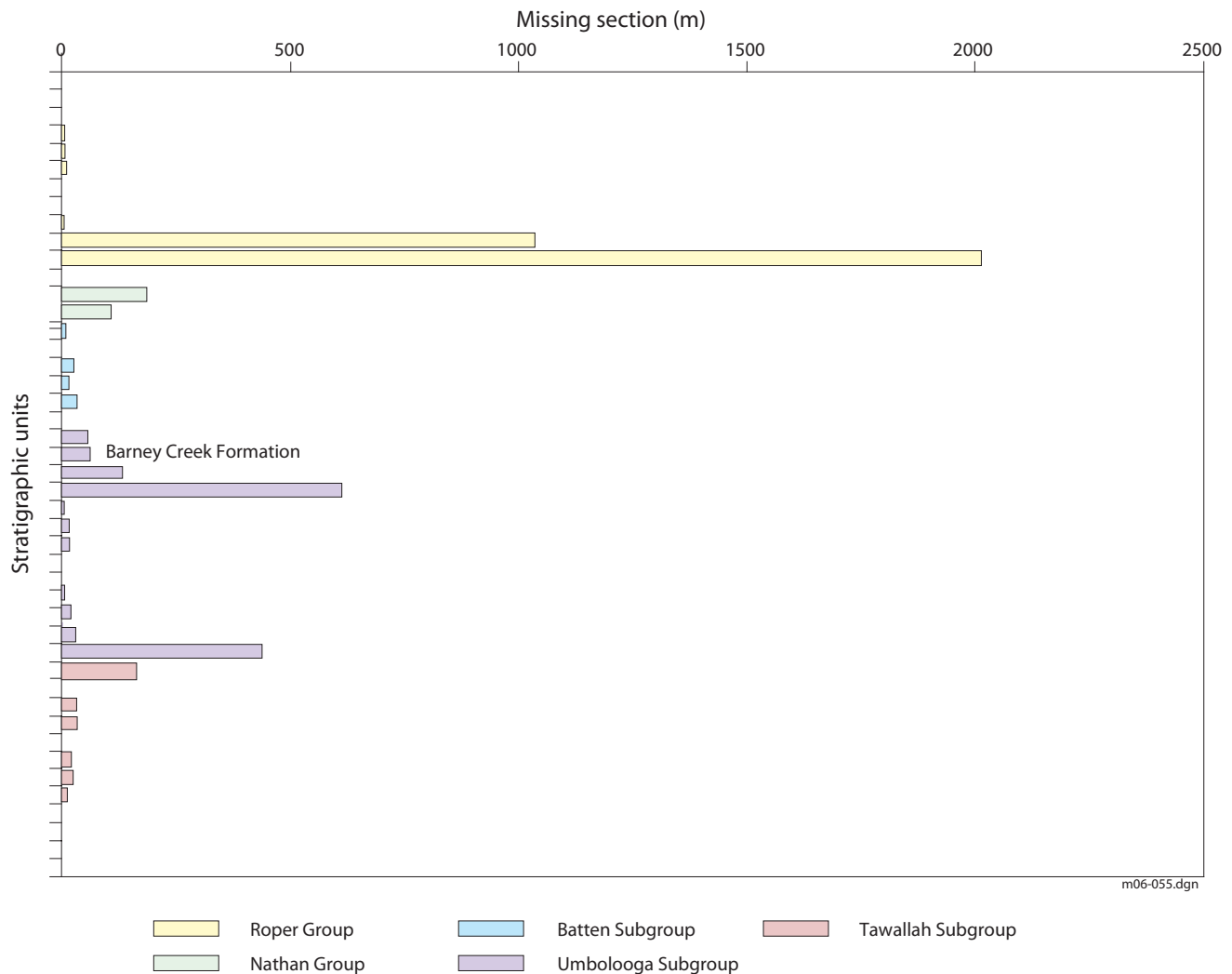


**Figure 12.** Volume of sediment absence/removal through time, as indicated by the average thickness of section missing at the base of McArthur Basin units. The mean value was calculated for each stratigraphic unit by  $\sum L_i M_i / C$  where  $C$  is the total length of all basal contacts of the stratigraphic unit,  $L$  is the contact length in metres (derived from the unconformity subset of the arc attribute table), and  $M$  is the thickness in metres of missing section (derived from the stratigraphic attribute table), for each mapped unconformable contact  $i$ . The bar denoting the base of the Barney Creek Formation, host unit of the HYC deposit, is labelled for reference.

mineralising fluids. Significant portions of the sediment originally filling the basin have subsequently been lost through deformation, uplift and erosion. This section presents a rapid, easily implemented procedure for inferring palaeo-basin structure. It builds on the method described above for estimating the depth to any basin unit, given the outcrop of a unit higher in the stratigraphy. The resulting map (exemplified by Figure 7), representing the stratigraphic depth dimension keyed to geological map polygons, is used as a baseline for comparison with the geophysically interpreted 2.5-D representation of present basin volume. Areas where the interpreted depth to the base of the McArthur Group carbonate package (Figure 5) is in excess of that predicted from outcrop geology are inferred to have been sub-basins, since the preserved basin sediment fill is anomalously thick. Conversely, regions where an anomalously thin volume of basin fill is preserved, with reference to the stratigraphic elevation of outcropping units, are interpreted to have been relatively elevated within the basin during deposition.

The technique relies on the assumption that basin strata dip only shallowly in the area considered. This is violated to a degree in some parts of the McArthur Basin, where

dips steepen up to 70° near faults (see discussion above), but these zones are not considered sufficiently extensive to invalidate the method as applied at 1:250 000 scale.

The McArthur Group carbonate portion of the basin fill (essentially comprising the entire group, except for the mainly siliciclastic Mallapunyah Formation and Masterton Sandstone at the base; hereafter referred to as the upper McArthur Group) is examined in this instance. The amount of section between the surface and the base of the upper McArthur Group is calculated for each McArthur Group polygon younger than the Mallapunyah Formation, from the difference between its related ZMEAN stratigraphic depth attribute and the ZMEAN corresponding to the base of the upper McArthur Group units (basal Amelia Dolostone). The resulting new stratigraphic attribute ('predicted upper McArthur Group thickness') describes in terms of thickness the amount of implied upper McArthur Group sediment between the outcropping unit and the base of the upper McArthur Group carbonate-dominated package.

A 100 m grid cell raster was created from the geology polygons and the predicted upper McArthur Group thickness attribute. This enabled comparison of upper

McArthur Group thickness predicted from surface geology with the geophysically interpreted present upper McArthur Group carbonate volume (Figure 5). It was assumed for this exercise that a full section of upper McArthur Group was present beneath the younger Proterozoic Nathan and Roper groups; thus, a nominal maximum predicted upper McArthur Group thickness value of 2650 m was assigned to these areas. Phanerozoic and pre-upper McArthur Group units (Mallapunyah Formation and older) were initially designated as null values.

Predicted upper McArthur Group thickness values were subsequently interpolated in areas of Phanerozoic cover using a three-stage procedure. The initial grid was first converted into a lattice of points, attributed with the predicted upper McArthur Group thickness value. A TIN was then created from these points, incorporating all faults as barrier lines. Finally this TIN was linearly interpolated back to a lattice, and areas of pre-upper McArthur Group outcrop covered by the interpolation masked out.

The resulting grid was subtracted from the grid representing present McArthur Group carbonate thickness, as interpreted by Leaman (1998), and the residual map of anomalous upper McArthur Group carbonate package thickness is shown in Figures 13a and b.

Figures 13a and b present a number of important features. The area adjacent to the Emu Fault from the Masterton Horst southwards shows the greatest anomalous thickness, but a significant portion of this is probably due to structural repetition and unusually steep dips in this complexly deformed zone. Of more significance is the overall anomalously thick area extending southwest from HYC across most of the region as far as the Tawallah Fault, forming a rough quadrilateral slightly elongated in an east–west direction. This feature is interpreted as a sub-basin (hereafter called the Hot Spring-Emu sub-basin) present in upper McArthur Group time, ie broadly contemporaneous with formation of the HYC deposit.

The fault boundaries of this sub-basin are interpreted as pull-apart structures associated with contemporaneous strike-slip movement on the Emu and Tawallah faults. These were potentially conduits for mineralising fluids. It is notable that most of the mineral deposits in the region are localised in the vicinity of these boundaries, which are distinguished by a comparatively rapid transition from anomalously thick to anomalously thin areas. The most prominent of these bounding zones extends westwards from just north of HYC, though it is embayed around 608000mE. This embayment is part of a low north–south-trending ridge, which partially bisects the Hot Spring-Emu sub-basin. It also is spatially associated with stratiform Zn-Pb mineralisation. The two basin cells on the western and eastern sides of the ridge are bounded on their far sides by the Hot Spring and Emu faults, respectively. Either may have acted as a reservoir for base metal-bearing fluids, prior to their release upwards along bounding faults or other discontinuities at the cell edges, accounting for the localisation of stratiform Zn-Pb mineralisation in suitable trap rocks in these areas.

Other sub-basins are identified in Figures 13a and b, though they do not appear as voluminous as the Hot Spring-Emu sub-basin. One is at the northern edge of the study area in the Sawtooth Range, where an anomalous thickness of upper McArthur Group is inferred to have existed. No Zn-

Pb mineralisation has yet been identified in this area, though suitable reducing trap rocks (Barney Creek Formation, Caranbirini Member) are present.

The area between the Foelsche Inlier and Hot Spring Fault in the southeastern corner contain only slightly anomalous patches of upper McArthur Group, which are considered either too small or too diffuse to have concentrated large amounts of mineralising fluids. Only one stratiform base metal prospect is known in this region (Mountain Home), and it is not known to contain significant Zn-Pb grades. Some of the more intensely anomalous features at the extreme southeastern edges of the maps in Figure 13 are interpolative edge artifacts arising from the lack of outcrop geological control in this area, which is largely covered by Cambrian sandstone of the Georgina Basin (Bukalara Sandstone).

## CONCLUSIONS

These GIS techniques enable semi-automatic generation of coverages representing ‘predicted’ structural elevation for any given stratigraphic unit, based purely on outcrop geology and measured stratigraphic thicknesses. The geological data were thus used to generate a baseline prediction for (present) basin geometry, by making the simplifying assumption of ‘layer cake’ stratigraphy. The resulting maps provide a quantitative visualisation of basin structure not obvious on casual inspection. They particularly emphasise the magnitudes of vertical displacements across faults.

A method for the automatic detection of unconformities in geological maps was developed, which utilised the GIS topological data structure and a look-up table based on the stratigraphic column. This method was extended to calculate the ‘magnitude’ or thickness of missing sedimentary section represented by each unconformity. The resulting unconformity map clearly indicates areas of uplift or low subsidence during basin development, where stratigraphic units are absent due to erosion or lack of deposition, or both. The unconformity magnitude indicates the extent and persistence of locally elevated regions within the basin, while the relative age of the missing units gives an indication of the time during which these features were present. Pre-Roper Group uplift increasing in magnitude to the south is highlighted, as are instances of missing section within the Umbolooa Subgroup, to the west and south of HYC.

A geophysically derived model for the thickness of the McArthur Group was subtracted from a model of ‘predicted McArthur Group thickness’, derived purely from outcrop geology to produce a map depicting areas of ‘anomalously high’ or ‘anomalously low’ thickness. These zones may be directly interpreted as representing sub-basins and relatively elevated areas present during McArthur Group time. This basin geometry is inferred to have exerted a direct influence on basin fluid flow at the time the HYC ore deposit was formed. The HYC deposit is located at the northeastern corner of the largest sub-basin identified, the Hot Spring-Emu sub-basin, which is composed of two elongated cells on either side of a shallow central ridge. Stratiform Zn-Pb mineralisation is spatially associated with the edges or shoulders of the sub-basin cells. Other palaeo-sub-basins are present, but these are not as voluminous and are not spatially associated with currently known significant Zn-Pb occurrences.

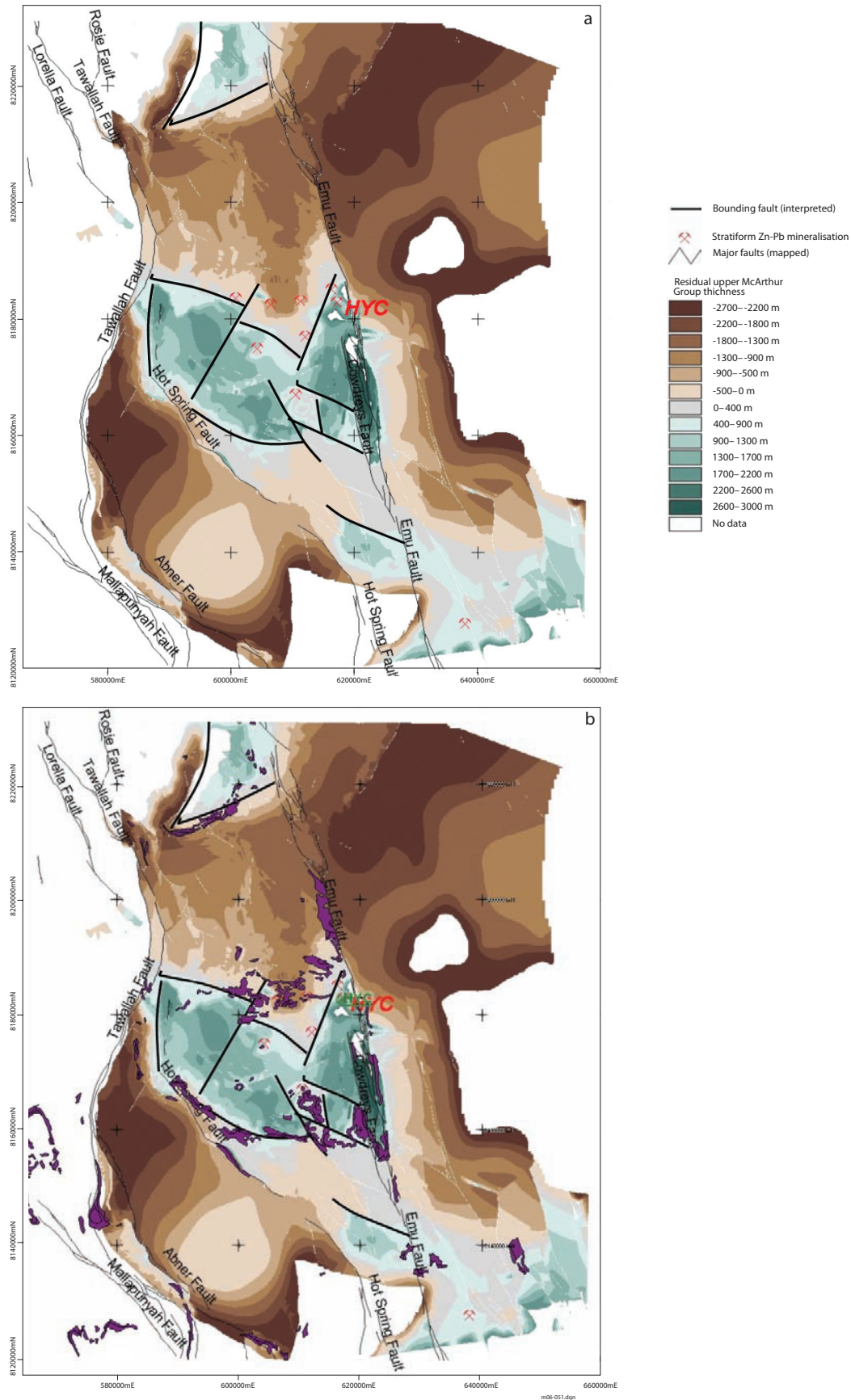


**Figure 13.** (a) Residual upper McArthur Group thickness, calculated by subtracting presumed current thickness of upper McArthur Group units implied by outcrop geology from the interpreted preserved thickness of McArthur Group. Negative values (brown shades) thus denote areas where there is less upper McArthur Group preserved than would be expected in a 'normal' sedimentary section, and are interpreted as areas which were elevated during upper McArthur Group deposition. The reverse applies to areas of positive residual values, which are interpreted as palaeo-sub-basins. (b) the same figure with an additional overlay of outcrops of units known to contain reducing shale 'trap' lithologies (purple). The thicker fault lines shown are interpreted syn-sedimentary structures.



# REFERENCES

- Blewett R, 1993. The AGSO field geological note books – a user's guide. *Australian Geological Survey Organisation, Record* 1993/94.
- Bonham-Carter GF, Agterberg FP and Wright DF, 1990. Weights of evidence modelling: a new approach to mapping mineral potential: in Agterberg FP and Bonham-Carter GF (editors) 'Statistical Applications in the Earth Sciences.' *Geological Survey of Canada, Paper* 89-9, 171–183.
- D'Ercole C, Groves DI and Knox-Robinson CM, 2000. Using fuzzy logic in a Geographic Information System environment to enhance conceptually based prospectivity analysis of Mississippi Valley-type mineralisation. *Australian Journal of Earth Sciences* 47, 913–927.
- Duffett ML, 2000. *Geophysical and GIS applications to exploration for Proterozoic sediment-hosted Zn-Pb mineralisation, northern Australia*. PhD thesis, University of Tasmania.
- Duffett ML and Leaman DE, 1997. McArthur Basin architecture – a new perspective from geophysics and GIS. *Exploration Geophysics* 28, 39–42.
- Dunster JN, 1996. Sedimentology of the Lady Loretta Formation – a comparison of the regional setting to that of the Lady Loretta orebody: in Baker T *et al* (editors) 'MIC '96: The McArthur, Mt Isa, Cloncurry Minerals Province – New Developments in Metallogenic Research, Extended Conference Abstracts.' *EGRU Contribution* 55, 47–50.
- Etheridge MA, Rutland RWR and Wyborn LAI, 1987. Orogenesis and tectonic process in the early to middle Proterozoic of northern Australia: in Kroner A (editor) 'Proterozoic Lithospheric Evolution.' *Geodynamics Series* 17, 131–147. American Geophysical Union, Washington DC.
- Etheridge M and Wall V, 1994. Tectonic and structural evolution of the Australian Proterozoic. *12th Australian Geological Convention, Geological Society of Australia, Abstracts* 37, 102–103.
- Hinman M, 1996. Constraints, timing and processes of stratiform base metal mineralization at the HYC Ag-Pb-Zn deposit, McArthur River: in Baker T *et al* (editors) 'MIC '96: The McArthur, Mt Isa, Cloncurry Minerals Province – New Developments in Metallogenic Research, Extended Conference Abstracts.' *EGRU Contribution* 55, 56–59.
- Hinman M, Wall V, and Heinrich C, 1994. The interplay between sedimentation, deformation and hydrothermal activity at the McArthur Pb-Zn (-Cu) deposit. *12th Australian Geological Convention, Geological Society of Australia Abstracts* 37, 176–177.
- Jackson MJ, Muir MD and Plumb KA, 1987. Geology of the southern McArthur Basin, Northern Territory. *BMR Bulletin* 220.
- Jackson MJ, Sweet IP and Powell TG, 1988. Studies on petroleum geology and geochemistry of the middle Proterozoic McArthur Basin, northern Australia I: petroleum potential. *Australian Petroleum Exploration Association, Journal* 28, 283–302.
- Knox-Robinson CM, Robinson DC and Groves DI, 1992. The use of geographical information systems as a gold prospectivity mapping tool, with reference to the Yilgarn Block, Western Australia: Requirements and limitations: in Geological Applications of Geographic Information Systems (GIS). *Australian Institute of Geoscientists, Bulletin* 12, 71–82.
- Large RR, Bull SW, Selley D, Yang J, Cooke DR, Garven G and McGoldrick PJ, 2002. Controls on the formation of giant stratiform sediment-hosted Zn-Pb-Ag deposits: with particular reference to the north Australian Proterozoic: in Cooke, DR and Pongratz J (editors) 'Giant Ore Deposits: Characterization, Genesis, and Exploration.' *CODES Special Publication* 4, University of Tasmania, Hobart.
- Leaman DE, 1994. Criteria for evaluation of potential field interpretations. *First Break* 12, 181–191.
- Leaman DE, 1996. Are thick volcanic piles concealed in north Australian Proterozoic basins? *Exploration Geophysics* 27, 13–20.
- Leaman DE, 1997. Application of magnetic methods to deep basin structures. *Exploration Geophysics* 28, 97–105.
- Leaman DE, 1998. Structure, contents and setting of Pb-Zn mineralisation in the McArthur Basin, northern Australia. *Australian Journal of Earth Sciences* 45, 3–20.
- McClenaghan MP, Roach MJ and Bottrill RS, 1994. Structure of the GIS databases. *Mineral Resources Tasmania, Report* 1994/07 (unpublished).
- McGoldrick P and Large R, 1998. Proterozoic stratiform sediment-hosted Zn-Pb-Ag deposits. *AGSO Journal of Geology and Geophysics* 17(4), 189–196.
- Neudert M and McGeough M, 1996. A new tectonostratigraphic framework for the deposition of the upper McArthur Group, NT: in Baker T *et al* (editors) 'MIC '96: The McArthur, Mt Isa, Cloncurry Minerals Province – New Developments in Metallogenic Research, Extended Conference Abstracts.' *EGRU Contribution* 55, 90–93.
- Oehler JH and Logan RG, 1977. Microfossils, cherts and associated mineralization in the McArthur Deposit, NT, Australia. *Economic Geology* 72, 1393–1409.
- Page RW, Jackson MJ and Krassay AA, 2000. Constraining sequence stratigraphy in north Australian basins: SHRIMP U-Pb zircon geochronology between Mt Isa and McArthur River. *Australian Journal of Earth Sciences* 47, 431–459.
- Pietsch BA, Rawlings DJ, Creaser PM, Kruse PD, Ahmad M, Ferenczi PA and Findhammer TLR, 1991. *Bauhinia Downs, Northern Territory (Second Edition). 1:250 000 geological map series explanatory notes, SE 53-03*. Northern Territory Geological Survey, Darwin.
- Plumb KA, Ahmad M and Wygralak AS, 1990. Mid-Proterozoic basins of the North Australian Craton – regional geology and mineralisation: in Hughes FE (editor) *Geology of the mineral deposits of Australia and Papua New Guinea. Volume 1. Australasian Institute of Mining and Metallurgy, Monograph* 14, 881–902.
- Plumb KA and Wellman P, 1987. McArthur Basin, Northern Territory: mapping of deep troughs using gravity and magnetic anomalies. *BMR Journal of Australian Geology and Geophysics* 10, 243–252.

- Rawlings DJ, 1994. Characterisation and correlation of volcanism in the McArthur Basin and Transitional Domain, NT: in Hallenstein CP (editor) 'AusIMM Annual Conference Technical Program Proceedings.' AusIMM Publication Series 5/94, 157–160.
- Rawlings DJ, 1999. Stratigraphic resolution of a multiphase intracratonic basin system: the McArthur Basin, northern Australia. *Australian Journal of Earth Sciences* 46, 703–723.
- Rawlings DJ, 2007. Evolution of the Redbank Package: in Munson TJ and Ambrose GJ (editors) 'Petroleum and mineral potential of central Australian basins. Proceedings of the Central Australian Basins Symposium (CABS), Alice Springs, Northern Territory, 16–18 August, 2005.' Northern Territory Geological Survey, Special Publication 2 (this volume).
- Rogers J, 1996. *Geology and tectonic setting of the Tawallah Group, southern McArthur Basin, Northern Territory*. PhD thesis, University of Tasmania.
- Scott DL, Rawlings DJ, Page RW, Tarlowski CZ, Idnurm M, Jackson MJ and Southgate PN, 2000. Basement framework and geodynamic evolution of the Palaeoproterozoic superbasins of north-central Australia: an integrated review of geochemical, geochronological and geophysical data. *Australian Journal of Earth Sciences* 47, 341–380.
- Southgate PN, Bradshaw BE, Domagala J, Jackson MJ, Idnurm M, Krassay AA, Page RW, Sami TT, Scott DL, Lindsay JF, McConachie BA and Tarlowski C, 2000. Chronostratigraphic basin framework for Palaeoproterozoic rocks (1730–1575 Ma) in northern Australia and implications for base-metal mineralisation. *Australian Journal of Earth Sciences* 47(3), 461–483.
- Wright DF and Bonham-Carter GF, 1992. Two case studies for mapping mineral potential using weights-of-evidence modelling: Gold in Meguma Terrane, Nova Scotia and base metals in Snow Lake area, Manitoba: in 'Geological Applications of Geographic Information Systems (GIS).' Australian Institute of Geoscientists, Bulletin 12, 83–84.
- Wyborn LAI, Gallagher R and Mernagh TP, 1995. Using GIS for mineral potential evaluation in areas with few known mineral occurrences. Proceedings of the Second National Forum on GIS in the Geosciences. *AGSO Record* 1995/46, 199–211.
- Yang Jianwen, Bull S and Large R, 2004. Numerical investigation of salinity in controlling ore-forming fluid transport in sedimentary basins: example of the HYC deposit, northern Australia. *Mineralium Deposita* 39, 1–19.

**Mark Duffett** majored in Geology and Geophysics at the University of Adelaide, then proceeded to Honours and a PhD in geophysics and GIS at the University of Tasmania. Following three years at Charles Darwin University working on a range of integrated GIS and remote sensing projects, including crocodile nesting habitat mapping, he joined NTGS as a geophysicist in 2001. There, he worked primarily on geophysical interpretation and 3D modelling aspects of projects in the Georgina Basin and eastern Arunta Region. He is now a research fellow in regional geophysics at the ARC Centre of Excellence in Ore Deposits (CODES), University of Tasmania.



**Michael Roach** is a lecturer in geophysics and geology in the School of Earth Sciences and the CODES Centre of Excellence at The University of Tasmania. Prior to joining the University of Tasmania, he worked for nine years with BHP in exploration and mining geology, principally in the coal industry. Michael's research focuses on potential field data interpretation, environmental geophysics and petrophysical studies of mineralised systems.



**David Leaman** received a BSc (Hons) and PhD from the University of Tasmania. From 1966 to 1981, he worked for the Geological Survey of Tasmania on many applied geophysical, hydrological and structural projects. Since mid 1981, he has been a consultant, specialising in the application of gravity and magnetic methods to the appraisal of structural setting and control of ore deposits, coal and petroleum basin studies, basin evolution and certain classes of engineering studies. He has wide experience within Australia and was a contract senior lecturer in Geophysics, Tectonics and Environmental topics at the Centre for Ore Deposit and Exploration Studies at the University of Tasmania from 1972-2001. He is a member of ASEG, EAEG, PESA and GSA.

